FAERE
French Association
of Environmental and Resource Economists

Working papers

Crop Prices and Deforestation in the Tropics

Nicolas Berman – Mathieu Couttenier – Antoine Leblois – Raphael Soubeyran

WP 2022.08

Suggested citation:

N. Berman, M. Couttenier, A. Leblois, R. Soubeyran (2022). Crop Prices and Deforestation in the Tropics.
FAERE Working Paper, 2022.08.

ISSN number: **2274-5556**

www.faere.fr

Crop Prices and Deforestation in the Tropics*

Nicolas Berman† Mathieu Couttenier ‡ Antoine Leblois § Raphael Soubeyran ¶

November 8, 2022

Abstract

Global food demand is rising, driven by a growing world population and dietary changes in developing countries. This situation encourages farmers to increase crop production which, in turn, increases worldwide demand for agricultural land and the pressure on tropical forests. Given the probability that growth in world food demand will continue, this pressure is not likely to abate in coming decades. While the impact of food demand on deforestation has been in the headlines, rigorous evidence of the relationship between international crop prices and deforestation using large-N data remains scarce. We attempt to quantify this link during the twenty-first century using high-resolution annual forest loss data for tropical regions, combined with information on crop-specific agricultural suitability and annual global commodity prices. We find that price variation has a sizable impact on deforestation: crop price increases are estimated to be responsible for a third of the total deforested area in the tropics (approx. 2 million km^2) during the period 2001-2018. We also find that the degree of openness to international trade and level of economic development are first-order local characteristics affecting the magnitude of the impact of crop prices on deforestation.

*The data and the codes that generate the findings are openly available at https://zenodo.org/record/7044013. The project leading to this publication has received funding from the French government under the "France 2030" investment plan managed by the French National Research Agency (reference: ANR-17-EURE-0020) and from Excellence Initiative of Aix-Marseille University - A*MIDEX. Mathieu Couttenier acknowledges financial support from the IDEXLYON, University of Lyon (French National Research Agency, Programme Investissements d'Avenir, ANR-16-IDEX-0005)

†Aix Marseille Univ., CNRS, AMSE, Marseille, France, and CEPR. E-mail: nicolas.berman@univ-amu.fr.

‡ENS de Lyon & CEPR. E-mail: mathieu.couttenier@ens-lyon.fr

§CEE-M, Univ. Montpellier, CNRS, INRAE, Institut Agro, Montpellier, France. E-mail: antoine.leblois@inrae.fr.

¶CEE-M, Univ. Montpellier, CNRS, INRAE, Institut Agro, Montpellier, France. E-mail: raphael.soubeyran@inrae.fr.

1 Introduction

Tropical deforestation is one of the main causes of global environmental changes. Recent estimates indicate that food systems are responsible for a third of global anthropogenic GHG emissions (Crippa et al., 2021) and that 17% of tropical moist forests have disappeared since 1990, with a remaining area of about one billion hectares as of 2019, of which 10% are degraded (Vancutsem et al., 2021). Deforestation threatens crucial ecosystem services, such as biodiversity richness, climate regulation, carbon storage and water supplies, and encourages the spread of infectious diseases.[1] Curbing deforestation not only provides private goods such as forest timber and non-timber products, local public goods in terms of watersheds, erosion control, nutrient recycling and local climate effects, but also global public goods such as carbon storage and biodiversity (e.g. Sandler 1993). The main market failure comes from the global public goods and the positive externalities that preservation efforts of one country provides to the other countries. These externalities are hardly valued by market forces which are among the most prominent determinants of tropical deforestation (Geist and Lambin, 2002; Curtis et al., 2018; Balboni et al., 2022), since they are largely responsible for driving agricultural expansion (Angelsen, 1999; Pendrill et al., 2019). Forecasts point to a sharp increase in food demand in coming decades, with projected growth of at least 50% by 2050 (Fukase and Martin, 2020; FAO, 2017). This will clearly drive crop prices up and also likely leading to a strong increase in the demand for land, which in turn will increase the private value of agricultural land (Souza-Rodrigues, 2019).

In this paper, we estimate the effect of changes in crop prices on deforestation in the tropics. We combine various datasets for the tropical regions at the spatial resolution of 0.5 degree latitude and longitude grid cells (approximately 55 $\times$ 55 kilometers at the equator) for the period 2001-2018. First, we make use of fine-grained estimates of yearly deforestation at the level of 1 arc-second pixels (approximately 30 meters $\times$ 30 meters at the equator) (Hansen et al., 2013). For each cell, we compute the total number of pixels that are deforested in each year. Second, we gather cell-specific information on the agronomic suitability of 15 crops in order to proxy the potential crop specialization at the cell level (Global Agro-Ecological Zones, GAEZ hereafter, Fischer et al., 2012). We combine these data with the international prices of crops traded on international markets in order to construct a cell-specific, time-varying crop price index. This index is computed as the weighted sum of the international crop prices in a given year, weighted by the relative agronomic suitability of each crop in the cell (Methods in Section 3.1 and Online Appendix, hereafter OA, – Section OA1.1 and OA1.2). Our final sample includes around 12,000 cells of 0.5 $\times$ 0.5 degree, over the period 2001-2018.

Our identification strategy exploits within-cell variation in the crop price index and deforestation over time. We control for a large array of unobserved factors, namely all time-invariant cell characteristics, national time-varying shocks that might correlate with both deforestation and international crop prices, and local shocks such as weather fluctuations. We find that changes in crop prices significantly affect deforestation in the tropics and that the effect is sizable: our baseline estimates imply that increase in

[1] See Foley et al. (2005); Turner et al. (2007); Le Quéré et al. (2016); Alkama and Cescatti (2016); Song et al. (2018); Chaves et al. (2020); Tollefson (2020).

our price index observed explains around a third of the total deforestation observed in the tropics over the period (i.e. approx. 2 million km^2). The effect of international price variations on deforestation significantly increase with initial forest cover, and it depends on cell-specific characteristics. The estimates are magnified in cells more opened to international trade (proxied by the distance to seaports), in poorer areas (proxied by nighttime luminosity in 2000) and, to a lesser extent, in areas with weaker state capacity (proxied by the distance to the capital city). Our results are robust to a variety of sensitivity tests, including the use of different estimators, standard errors adjustments, various definitions of the canopy threshold, inclusion of additional controls which may affect both deforestation and prices, or the exclusion of large traders which could influence world commodity prices. While our results could be driven only by a direct effect-international prices directly affecting actors such as multinationals, states, or local land managers, we provide suggestive evidence that they are also driven by an indirect effect-international prices affecting deforestation through their effect on local prices. Using data on a sub-sample of countries and crops, we find that local crop prices indeed correlate substantially with international prices. We interpret our results as demand-driven, as we perform a number of robustness checks that suggest that supply conditions in large producers do not affect the estimates. We further strengthen this interpretation by showing that our results are qualitatively similar when using, instead of our international prices index, a measure of foreign demand based on changes in foreign imports. Hence, our results suggest that changes in global demand, and modifications of individual preferences may have strong impact on deforestation levels.

Our paper contributes to the literature in different dimensions. First, this paper is the first attempt to estimate the effect of crop prices on deforestation at the local level on a global scale. While the idea that international crop prices, driven by expanding global demand, are contributing to tropical deforestation is not new (Angelsen, 1999; Angelsen and Kaimowitz, 1999; Angelsen, 2010; Rudel et al., 2009; Busch and Ferretti-Gallon, 2017), the empirical evidence to date has a number of drawbacks. Either it is based largely on cross-national comparisons; it focuses on a single country or region; considering only a limited number of commodities, or focusing on a short period of time (Pendrill et al., 2022).[2] The usual approaches in the studies carried out on a global scale include spatial attribution, input-output, and trade and land-balance modeling.[3] These approaches typically use supply-side models at the national level and downscale national trade or production data to the local level. Second, by using worldwide information on agricultural suitability based on resource limitations (plant eco-physiological characteristics, climatic and edaphic requirements of crops), our approach is more tractable and aims to overcome the absence of fine-grained information in many poor countries.[4] Third, our methodology is agnostic in terms of scale of agricultural

[2]For papers related to cross-national comparisons, see Angelsen and Kaimowitz (1999); Rudel et al. (2009); DeFries et al. (2010); Hosonuma et al. (2012); Ordway et al. (2017); Leblois et al. (2017); related to a single country or region Barbier and Burgess (1996); Gaveau et al. (2009); Wheeler et al. (2013); Hargrave and Kis-Katos (2013); Assunção et al. (2015); Faria and Almeida (2016); Doggart et al. (2020); Harding et al. (2021); Fehlenberg et al. (2017); Ordway et al. (2017); Lundberg and Abman (2021); related to a limited number of commodities, see Goldman et al. (2020).

[3]For papers related to spatial attribution, see Goldman et al. (2020); Curtis et al. (2018); Austin et al. (2019); related to input-output, see Godar et al. (2015); Green et al. (2019); Hoang and Kanemoto (2021); related to trade and land-balance modeling, see Pendrill et al. (2019); Henders et al. (2015); Pendrill et al. (2019).

[4]National data have well-known limitations. They are subject to omission bias stemming from undeclared activities, such as home-based and locally-consumed agricultural production. A large share of small-holder production is consumed locally and not traded on international markets, such as oil in Sub-Saharan Africa (Ordway et al., 2019). Trade flow analyses and

production, in contrast to studies based on spatial attribution or classifications methods, which attribute large-scale commodity-driven deforestation to shifting agriculture (Curtis et al., 2018; Austin et al., 2019).[5] Fourth, it makes use of a sample of areas that were forested at the beginning of the sample period, rather than areas that are deforested at the end of the period, thus facilitating causal interpretation. Fifth, our empirical approach that combines exogenous local crop suitability with global crop prices allows us to control for a wide range of potential confounding factors not accounted for in previous studies. Finally, we highlight a number of policy-relevant local factors affecting the way in which fluctuations in crop prices trigger deforestation.

The remainder of the paper is organized as follows. Section 2 discusses the potential mechanisms, while Section 3 describes the data and the empirical strategy. Section 4 presents the results. Section 5 displays the main sensitivity analysis and discuss in length the interpretation of our results. Finally, Section 6 concludes.

2 International prices and local deforestation - mechanisms

Average effect. Our objective is to estimate how international crop prices affect local deforestation. Our claim is that land managers are heterogeneously exposed to crop price movements, depending on how suitable local land is for producing these commodities. In other words, fluctuations in the international price of, say, rice, primarily affect areas suitable for growing rice and the decision of land managers to cut the forest in this place. Differences across locations in the intensity of exposure to specific commodity price movements may generate different deforestation patterns. International crop prices may affect local deforestation through several channels. First, world prices may affect land use decisions of local producers through local markets and local prices. This mechanism is likely to be prevalent if farmers sell their crops locally, and if local and international markets are sufficiently integrated. The local presence of multinational companies, for whom international prices matter most and that may buy a significant part of the production may also represent an important driver of the transmission of the international prices to local prices. However, trade barriers (trade costs, tariffs...), supply chain frictions, and high shares of local demand may translate into a weak correlation between the international and local prices. We discuss this point in Section 5.2, where we use a sub-sample of locations to study the correlation between local and international crop prices. Second, a surge in the international price may push multinational firms to invest massively in crop production leading to deforestation, especially in food crops. Third, increases in international prices may push countries to relax the constraints (e.g. legal and tax systems) to ease deforestation. Alternatively, countries may decide to subsidize the agricultural sector to promote land changes toward crop production. In all cases, international price surge act as push factor of deforestation and not only through local prices.

trade accounting methods are also limited by their lack of spatial explicitness, leading to imprecise links between consumption patterns and socio-environmental impacts in production regions (Godar et al., 2015).

[5]Because they rely on the recognition of spatial patterns, these methods cannot be used to link production of – or demand for – commodities to small-scale deforestation that may also be, directly or indirectly, related to demand in international markets.

Local factors. Though our methodology primarily relates local crop-specific agronomic suitability to deforestation, other local factors may play a role. First, and as suggested in the literature (Ferreira, 2004; Souza-Rodrigues, 2019; Abman and Lundberg, 2020), we expect openness to international trade to exacerbate the role played by crop prices. In areas naturally more open to trade – e.g. those closer to seaports –, land managers should respond more to variations in international commodity prices. Second, local institutional quality and the capacity of states to enforce property rights may also affect the sensitivity of deforestation to crop prices (Angelsen, 1999). Indeed, under open access regimes, for instance, rational farmers should theoretically rush to exploit land and cut forest more quickly (Chichilnisky, 1994; Ferreira, 2004). The impact of the formalization of land rights and land tenure on forest loss has been demonstrated in the case of a land registration program in Benin (Wren-Lewis et al., 2020), in the case of a land titling program in the Brazilian Amazon (Probst et al., 2020) and with respect to the effect of customary tenure systems on deforestation which has been shown in the case of Cameroon (Ordway et al., 2017). Using local-level proxies of trade openness and state capacity, we study how these characteristics affect the link between international crop prices and deforestation in Section 4.2.

3 Data and Empirical Strategy

3.1 Data

We consider a full set of grid cells for the tropics, i.e. the area between the Tropic of Cancer at 23°26' N and the Tropic of Capricorn at 23°26' S, divided in sub-national units of 0.5×0.5 degrees latitude and longitude (approximately 55×55 kilometers at the equator). The unit of observation in our dataset is a cell-year; that is, we estimate how increases in crop prices affect deforestation in a given cell during a given year, over the 2001-2018 period.

Deforestation. We use the tree cover loss data from Hansen et al. (2013), which is based on Landsat data. They define tree cover loss as a stand-replacement disturbance or the complete removal of tree cover canopy at the pixel scale.[6] The original data contain an estimation of the annual tree cover loss for the period 2001-2018 (Online Appendix, hereafter OA, Section OA1.1), relative to the 2000 forest cover, for pixels at a spatial resolution of 1 arc-second (around 30 meters). For the baseline estimates, we consider a 1 arc-second pixel as being a forest when the forest cover in year 2000 is greater than 25%, as in other global studies using the same data (Heino et al., 2015; Potapov et al., 2008; Hansen et al., 2010). In the sensitivity analysis, we use a 50% canopy threshold (Section OA2.6). For each of these thresholds, we count the number of pixels defined as deforested within each 0.5×0.5 degrees cell-year. For our baseline measure of deforestation, we consider only cells with more than 5000 pixels of cover in 2000 (i.e. more than 0.125% of the cell's area). Figure OA.1 shows the accumulated deforestation for each pixel during the sample period.

[6] Note that our data methodology does not, however, capture forest degradation, which has been shown to be surpassing deforestation in the Brazilian Amazon (Matricardi et al., 2020), and affects 10% of tropical moist forests (Vancutsem et al., 2021).

Crop Price Index. We make use of information on global crop prices and agronomic suitability to construct our price index. The index is based on information for 15 crops that traded on international marketplaces and for which data on both annual global prices and agronomic suitability are available: banana, barley, cocoa, coconut, coffee, cotton, maize, palm oil, rice, sorghum, soybean, sugar, tea, tobacco and wheat. Global crop prices (base 100 in 2000) are obtained from the World Bank Commodity Dataset (World Bank Group, 2020). Data on time-invariant agronomic suitability are obtained from the Global Agro-Ecological Zones (FAO, Fischer et al. (2012)).[7] Agronomic suitability is defined as the percentage of the maximum yield that can be attained in each grid cell. For each cell, we compute the cell-specific *relative* suitability of the crop (α_c^i) by dividing the suitability of the crop (S_c^i) by the sum of the suitability of all the crops as follows:

$$\alpha_c^i = \frac{S_c^i}{\sum_{j=1}^{15} S_c^j}, \tag{1}$$

Then, for each cell c and year t, we compute our price index of crops based on the cell-specific relative suitability of each crop i.

$$\text{Price}_{c,t} = \sum_{i=1}^{15} \alpha_c^i \times P_t^i, \tag{2}$$

where P_t^i is the average worldwide price of crop i in year t.

Figure OA.4 and OA.5 and Table OA.2 uncover different summary statistics and detail the different sources of our identifying variations in our price index. First, there are striking cross-cell differences in the average price index variation over the 2001-2018 period (Figure OA.4). Second, for all crops, there is a substantial variation of prices over time – e.g., the two recent spikes related to the 2007-2008 and 2011-2012 world food price crises (Figure OA.5). Third, while positive overall, price correlations between crops are highly heterogeneous: from 4.3% between sugar and oilpalm to 96% between sorghum and maize (Table OA.2). Fourth, the share of the total variance of suitability coming from within country variation for each crop is substantial (Table OA.1). It ranges from 50% for tobacco to 74% for coconut. Altogether, variations in $\text{Price}_{c,t}$ are substantial even after conditioning on country and year fixed effects, as we shall do in our baseline methodology.

Final Sample. Our final sample covers the period 2001-2018 and is composed of 12,288 cells for which agronomic suitability data is available and forest cover in 2000 was strictly positive, i.e. at least 1 arc-second pixel is forest when the canopy threshold is larger than 25% of the cover. Our dataset is therefore a balanced panel of 221,184 observations. Tables OA.3 reports summary statistics about the main variables used in our study, including initial forest cover, deforestation and the price index $\text{Price}_{c,t}$.

3.2 Empirical strategy

We consider three alternative models. In Model 1, we estimate the impact of the log of the crop price index ($\ln \text{Price}_{c,t}$) on the inverse hyperbolic sine transformation of the number of deforested pixels ($\text{Deforest}_{c,t}$)[8] in cell c in year t, while controlling for cell and for country $\times$ year fixed effects (η_c and

[7] GAEZ, FAO data, available http://www.fao.org/nr/gaez/about-data-portal/en/

[8] This transformation is frequently used as it approximates the natural logarithm while allowing for zero-valued observations in the estimation (Burbidge et al., 1988; MacKinnon and Magee, 1990; Pence, 2006).

$\nu_{country,t}$, respectively):

$$\text{Deforest}_{c,t} = \beta \ln \text{Price}_{c,t} + \eta_c + \nu_{country,t} + \varepsilon_{c,t}, \tag{3}$$

where $\varepsilon_{c,t}$ is the error term. Standard errors are clustered by cell in the baseline, and in our sensitivity analysis we allow for spatially correlated errors within a larger radius. The inclusion of cell fixed effects control for any time-invariant cell characteristics that may correlate with both the average deforestation rates and crop prices (such as geography, topography and soil characteristics). The inclusion of country $\times$ year fixed effects ($\nu_{country,t}$) accounts for any time-variant country characteristics, such as global trends in overall crop prices, nationwide shocks or policy changes that may trigger or hamper deforestation. Since deforestation is bounded by the initial forest cover, we allow the effect of price ($\ln \text{Price}_{c,t}$) to vary across deciles of forest cover throughout the analysis (Model 2). We also allow it to vary across countries (Model 3) when looking at the effect of cell characteristics. We estimate the models using an Ordinary Least Square (OLS) estimator in the baseline estimations and a Poisson Pseudo Maximum Likelihood (PPML) estimator in the sensitivity exercises. Finally, to study the role of local characteristics we estimate equation (3) augmented with interaction terms between $\ln \text{Price}_{c,t}$ and cell-specific proxies of trade openness, development or state capacity (Section 4.2).

Identifying assumptions. In Section 5.1, we explore the sensitivity of our results to our various methodological choices – estimators, definitions of deforestation, lagged prices – and across sub-samples of data – regions, outliers, etc. Arguably more importantly, we provide a number of exercises supporting our causal interpretation of the results.

So far, we have interpreted β as an estimate of the impact of international prices variations on deforestation. This interpretation would fail if local prices are affected by deforestation and impact international prices, or if omitted variables which are cell-specific and vary over time affect deforestation and world prices. We show that our results are unlikely to be driven by reverse causality – local prices affecting world prices –: removing countries which account for a non-negligible share of world production leaves our results unchanged (Table OA.11 and OA.12). In addition, in our sensitivity exercises we will also control for local weather shocks, which may affect deforestation and local prices (Table OA.18).

Our price index is formed by suitability shares and international crop prices and we estimate the effect of variations of this index on deforestation at the cell-year level. Our empirical strategy can therefore be described as a shift-share ("Bartik") reduced-form approach. We have a very large number of cells (12,288) and a number of price shocks (15 crops x 18 years = 270) in our sample, and we include fixed effects. Following Goldsmith-Pinkham et al. (2020), the consistency of our estimator relies on the *exogeneity of the suitability shares to changes in deforestation within cells.* Though it is not directly testable, we believe that this is a plausible assumption. Forest cover (which conditions changes in deforestation) may indeed correlate with *absolute* suitability (S_c^i) – tropical forest grow on fertile soils. Yet, our methodology does not consider average suitability, but rather *relative* suitability in specific crops (α_c^i), which are arguably exogenous to deforestation variations. In Section 5.1 we provide series of robustness exercises that also support our causal interpretation.

4 Results

4.1 Crop prices and deforestation in the tropics

Our baseline results are represented graphically in Figure 1, and full estimations results are available in Table OA.4. We find that the cell-specific crop price index is positively and significantly correlated with deforestation ($\hat{\beta} = 1.27$, se $= 0.09$). The effect is seizable: a 10% increase in the price index leads to a 12.7% [±1.7pp] increase in deforestation (Figure 1, Model 1). As the potential for deforestation mechanically depends on the proportion of forest cover at the beginning of the period (Figure OA.2 presents forest cover in 2000), we allow the effect of crop prices to vary across deciles of cell-specific forest cover in 2000 (Figure 1, Model 2). For the first decile of cover, the point estimate is not significantly different from 0; then it triples from the second to tenth decile.[9]

Figure 1: Baseline effects of crop prices on deforestation

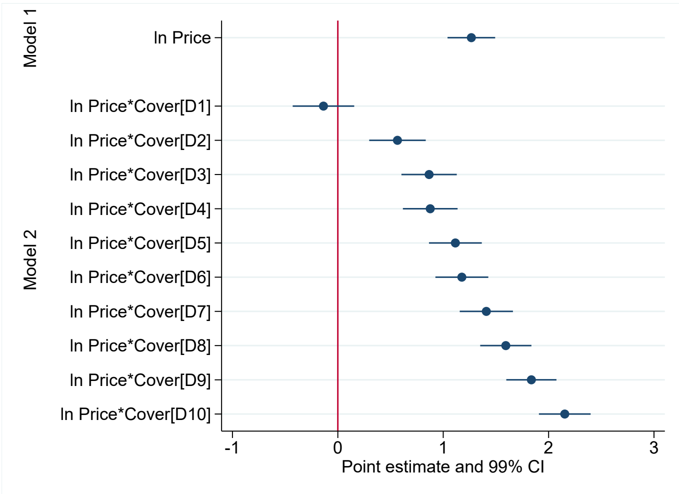

Note: Point estimates and confidence intervals for the effect of the crop price index on deforestation. Model 1 is the baseline estimate of the effect while Model 2 allows the effect of crops on deforestation to differ across deciles of forest cover as of 2000. Horizontal lines represent 95% confidence intervals. See Section 3 and Section OA2.1 for further details.

From 2001 to 2018, on average, the crop price index increased by more than 40% while the prices of specific leading crops, such as maize, rice, palm oil and soybeans, increased by between 45% and 85%. To get a sense of the role of the rise in crop prices on deforestation, we use the results presented in Figure 1, Model 2 to estimate the total contribution of crop price increases to deforestation during this period.[10] We find that the rise in crop prices was responsible for 35% of predicted global forest loss. Using the

[9] This result is not an artifact of the model specification. Though forest loss is bounded above by the decile of forest cover for each decile bin, in practice these bounds are never reached. To show this, we compute, for each grid cell, the number of deforested pixels over the total number of forest pixels at the beginning of the period for a canopy threshold of 25%, see Figure OA.3 in Section OA1.4.

[10] Our precise methodology is the following. Our aim is to compute the average contribution of crop prices variations over all the cells. For each cell, we proceed as follows. We first use the estimates from Model 2 (Figure 1) to compute the predicted level of deforestation, using observed prices (the benchmark). Second, we compute a counterfactual level of deforestation, using the same estimates but assuming that prices are fixed at their 2001 level. Third, we compute for each cell the contribution of prices variations as the difference between the benchmark and the counterfactual predictions, divided by the counterfactual.

PPML estimator rather than OLS leads to similar figures and average (Figure OA.11). As a comparison, Harding et al. (2021) find that a 56% increase in commodity prices led to a 19% increase in deforestation in Brazil over the 2004–2013 period.

Figure 2: Contribution of crop prices to deforestation, 2001-2018

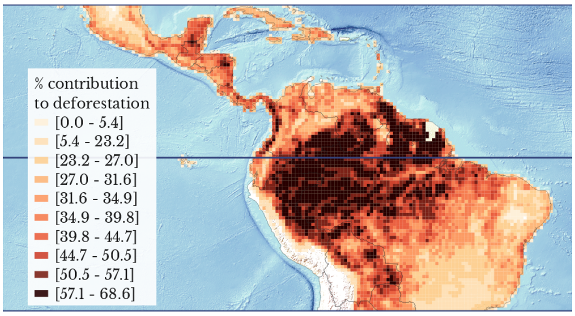

(a) Americas

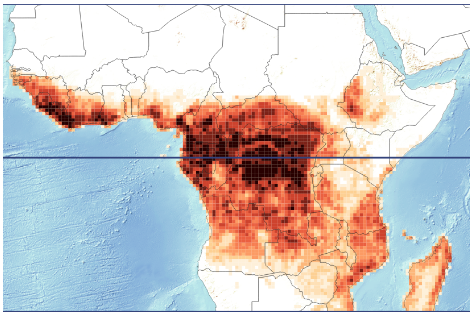

(b) Africa

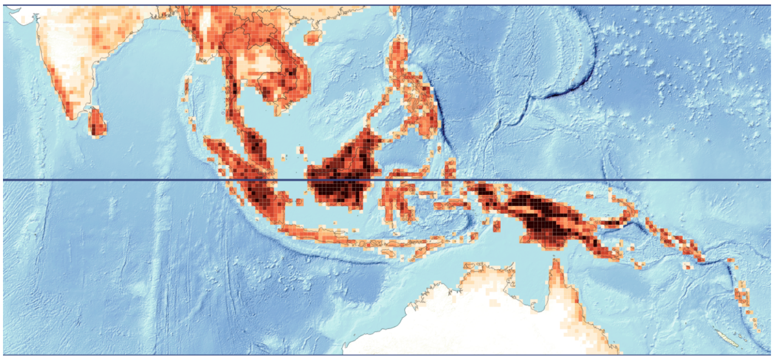

(c) Asia and Oceania

Note: Contribution of crop price increases to deforestation. Quantification based on the estimation results of Model 2 (see Section 3). We first compute the predicted level of deforestation using observed prices (the benchmark). We then compute a counterfactual level of deforestation assuming prices are fixed at their 2001 level. Finally, we sum these predictions by cell over the period and compute for each cell the contribution of prices as the difference between the benchmark and the counterfactual predictions, divided by the counterfactual.

Figure 2 shows the spatial heterogeneity across cells of the contribution of the crop price index variations to deforestation during the sample period. Differences across space are driven by (i) heterogeneous crop-specific suitabilities, and hence heterogeneous variations in global crop prices (Figure OA.4); (ii) the cell's initial forest cover (Figure OA.2). A visual inspection reveals that the contribution of the increase in international crop prices on deforestation has been the strongest in the three main tropical moist forest biomes: the Amazon, Southeast Asia and to a lesser extent West and Central Africa. Interestingly, we find that all tropical forests are subject to land pressure stemming from shocks to the prices of internationally traded commodities. Our results validate recent evidence indicating that despite cropland expansion in sub-Saharan Africa still being dominated by production for domestic markets, there is a growing influence of global markets on changing land use in the region (Ordway et al., 2017).

4.2 Trade costs and other local characteristics

As discussed in Section 2, local characteristics may dampen or exacerbate the contribution of crop price increases to deforestation. We consider two magnifying factors.[11] The first is international trade. In more open areas, land managers should be more impacted by changes in international prices. To measure the cell-specific exposure to international trade, we use information on the distance of the cell's centroid to the closest major seaport, as a proxy for transportation costs (Souza-Rodrigues, 2019). The second factor we consider is state capacity, or local institutional quality. We expect the effect of international crop prices on deforestation to be magnified in areas where the capacity of the state to enforce property rights is weaker. To measure institutional quality at the local level, we use the distance between the cell's centroid and the country's capital (Buhaug, 2010).[12] Rule of law, property rights protection and more generally institutional quality are expected to be weaker in places located far from the capital (Michalopoulos and Papaioannou, 2014). We also consider a measure of nighttime luminosity in 2000 (i.e. at the beginning of the sample period, to avoid reverse causality concerns) to proxy local economic development (Henderson et al., 2012; Bruederle and Hodler, 2018). State capacity and institutional quality are also expected to be stronger in wealthier locations. All cell-specific variables have been standardized to make coefficients comparable.

Figure 3: Cell-level characteristics

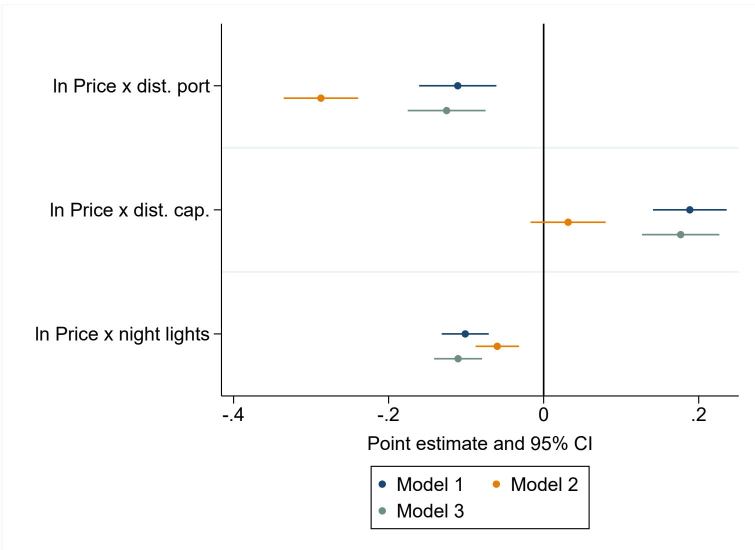

Note: The figure displays the point estimates and confidence interval of the effect of the interaction between cell-specific characteristics and our price index. The effect of crop price on deforestation is not reported here. Model 1 uses the baseline specification, augmented with interaction terms between the price index and (standardized) cell-characteristic variables (see Section 3 and Table OA.5). Model 2 allows the effect of crop price on deforestation to vary across the deciles of the initial forest cover distribution. Model 3 controls for a full set of interaction terms between country dummies and the price index.

[11] In Section OA2.5, we also consider heterogeneity at the country-level and include national differences in institutional quality, interacted with our crop price index. The coefficient estimates for these additional variables vary depending on the specification we consider. We discuss these results in Section OA2.5.

[12] While there is evidence, especially for African countries, that the power of the State diminishes outside the capital (Michalopoulos and Papaioannou, 2014), measuring local state capacity is still challenging. Among the different proxies (e.g. mountainous terrain (Hendrix, 2011), road density (Buhaug, 2006)), distance to the capital (Buhaug, 2010) is the most suitable for our purposes since it is the most exogenous and less related to international trade.

We consider each of the these potential mitigating factors by interacting the cell-specific characteristics with our price index in the baseline models. The standardized estimates of the interaction terms are plotted in Figure 3 (the full estimates are available in Table OA.5). Figure 3 considers three models: Models 1 and 2, as in Figure 1; and Model 3, which allows for heterogeneous effects of the price index across countries. In the latter model, we purge the estimates of the interaction terms of their country-wide component (e.g., differences in country size), focusing solely on within-country variation in cell characteristics.

First, we find that the positive effect of crop price increases on deforestation is significantly stronger in cells that are close to a seaport, suggesting that openness to international trade exacerbates the effect of crop price increases on deforestation. Second, and even though the significance of the estimates varies, the results point to larger commodity-driven deforestation in cells that are more distant from the capital city – i.e. locations with weaker state capacity. Finally, the effect of crop prices on deforestation is smaller in locations that are more economically developed. On average across specifications, distance to a port has the strongest effect. This provides support for the key role of access and exposure to international trade. The effect of trade costs and economic development remained virtually unaffected in our sensitivity checks, while the effect of local state capacity, measured by distance to the capital city, is less robust (see Section OA2.6).

Figure 4: Focus on the Congo Basin

(a) Baseline quantification

(b) Additional contribution of cell-level characteristics

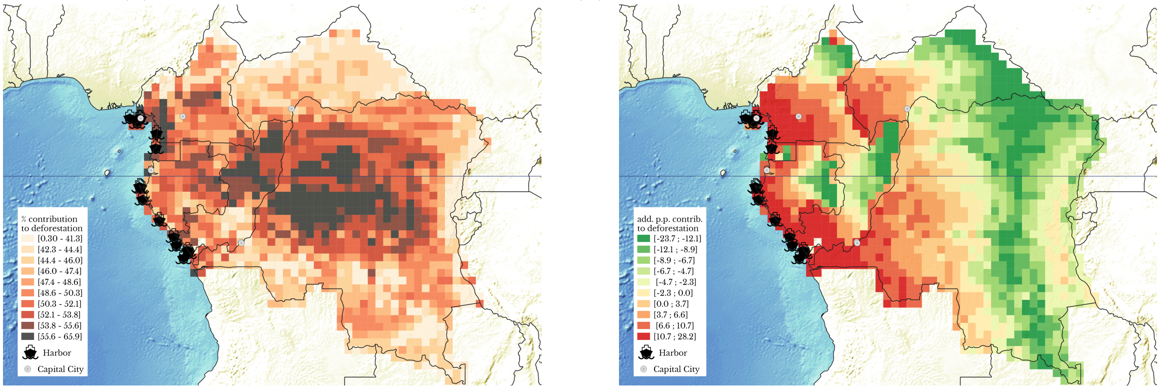

Note: Figure (a) shows the contribution of crop price increases to forest loss, with the sample restricted to the Congo Basin. Quantification is based on the estimation results of Model 2 (see Section 3). We first compute the predicted level of deforestation using observed prices (the benchmark). We then compute a counterfactual level of deforestation assuming fixed prices at their 2001 level. Finally, we sum these predictions by cell over the period and compute for each cell the contribution of prices as the difference between the benchmark and the counterfactual prediction, divided by the counterfactual. Figure (b) shows the difference in p.p. between Figure (a) and the sample quantification based on a specification where interaction terms between prices and cell characteristics are included (dist. port, dist cap. and light lights in 2000). For readability in brown and white, Figure b is reproduced with grey scale in Appendix Figure OA.6.

To illustrate these results, we focus on the Congo Basin, a major tropical moist forest biome spanning several countries. We first repeat the quantification exercise presented in Figure 2, restricting the sample to the countries of the Congo Basin. The results are shown in Figure 4.a, which displays for each cell the contribution of crop price increases to predicted deforestation during the sample period, as well as the location of major seaports and capital cities in each country. Second, we repeat this quantification exercise but use the specification that includes interactions with cell characteristics (Model 2 of Figure 3).

Figure 4.b plots the difference in percentage points between the two quantification exercises. Clearly, being close to a port has the strongest effect on commodity-driven deforestation. However, regions that are remote from the capital city also display significant differences, even though they are less exposed to international trade (e.g. the border between Cameroon and Central African Republic). A visual inspection of the same exercise for the full set of regions in the tropics delivers the same striking spatial patterns (Figure OA.7).

5 Robustness and Interpretation

5.1 Endogeneity concerns and sensitivity analysis

In Section 3.2, we mentionned the two main threats to our identification strategy. First, international prices may be affected by local prices, themselves impacted by deforestation or omitted local weather shocks. In other words, variations in our crop price index may be supply driven instead demand driven, and supply may correlate with deforestation. Second, the validity of our shift-share approach relies on the exogeneity of the suitability shares to changes in deforestation within cells. In this section, we discuss a number of tests which support a causal interpretation of our results.

Market power. We first show that reverse causality is unlikely to drive our results, i.e. that they are not reflecting the local conditions of countries with enough market power to influence international prices. Indeed, despite the fine-grained level of our analysis and the fact that we are using potential rather than actual agricultural production, we cannot completely rule out the possibility that deforestation and international commodity prices are simultaneously driven by supply-side shocks in major producing countries. For each country and crop, we compute the average market share of world trade during the sample period, and drop sequentially from the estimations countries belonging to the top 10%, 25% and 50% of our sample in terms of global market share. Our results remain largely unchanged when focusing only on small producers, which tends to confirm our demand-side interpretation of the results (Tables OA.11 and OA.12).

Confounding factors. Local weather shocks may affect both crop prices (through their effect on agricultural productivity) and deforestation (e.g. because wildfires are more likely in dry years). We add to our baseline specification the average cell-specific yearly temperature and the yearly total amount of precipitation. The results are largely similar to our baseline (Figure OA.18). Second, we control for the *absolute* level of agronomic suitability of the cell, which may affect both forest cover (hence the likelihood of deforestation) and crop prices (if cells with a higher absolute suitability are also more suitable for specific crops). If the land unsuitable for most crops in the sample is suitable for a crop that has relatively less positive price shocks (e.g., coffee) and also lacks forest cover, this may generate a spurious positive relationship between the price index and deforestation since increases in deforestation would necessarily occur where the crop price index has (relatively) large positive price shocks. Though such a correlation would be purely accidental, we can remove the concern by explicitly controlling for the average cell suitability ($\frac{1}{15}\sum_{j=1}^{15} S_c^j$) interacted with year dummies (controlling common price changes). This has little impact on our estimates - if anything, our baseline coefficient becomes slightly larger (Figure OA.12). Finally, in our baseline estimations we focus on agricultural crops and do not include meat in our price index. This may be a concern as studies have linked beef markets to Brazilian forest loss (Bowman, 2016) and land suitable for beef may also be suitable for crop production. To take beef production into account, we use GAEZ suitability data on alfalfa, pasture and grass together with data on the world price of beef from the World Bank. The methodology and the results are described in Section OA2.6.9 (Figures OA.14 and OA.15 and Tables OA.19 and OA.20). Our results are close to our baseline estimate.

Additional sensitivity analysis. All Tables and Figures related to the sensitivity analysis are relegated in Section OA2.6. First, using the number of deforested pixels as the dependent variable, we estimate our models using a Poisson Pseudo-Maximum Likelihood (PPML) estimator (columns 3 and 4 in Tables OA.7 and OA.8).[13] Second, we consider a different – more conservative – canopy threshold (50% instead of 25%) to ensure that 30m pixels contain enough tree cover in 2000 to be considered a forest biome (columns 1 and 2 in Tables OA.7 and OA.8). Third, we use the share of deforested pixels over forest cover at the beginning of the period as a dependent variable.[14] Our main result is qualitatively similar (Figure OA.13). Fourth, we ensure that our results are not driven by a small number of extreme observations by excluding observations that are 1, 2 and 3 standard deviations away from the residual mean (Tables OA.9 and OA.10). Fifth, we allow for both spatial and serial correlation, as the processes of deforestation and land conversion make it likely that the error term exhibits both spatial and serial correlation. We perform a non-parametric standard errors estimation (Conley, 1999; Hsiang et al., 2011), allowing for both cross-sectional location-specific serial correlation, as well as spatial correlation within a 500 or 1000 km radius (Tables OA.13 and OA.14). Sixth, we relax the assumption that price changes only have a contemporaneous effect on deforestation, by allowing the impact to be lagged (up to t -2) (Tables OA.15 and OA.16). Finally, we estimate the effect separately for South America, Africa and Asia and it again yields qualitatively similar results. In the case of South America, prices exhibit a stronger average impact on deforestation, but this is largely due to the fact that forest cover is higher on average in this case; for high levels of forest cover, the effect, though still larger in South America, becomes more uniform across regions (Table OA.17).

5.2 Mechanisms and interpretation

International prices and local prices. As mentioned in Section 2, several mechanisms can be at play to explain our results. In particular, while the effect of international crop prices on deforestation can be explained by local land managers (and countries) responding directly to changes in international prices, we believe that another mechanism -the transmission of international prices to local prices- is also at play and consistent with our results. Indeed, using household-level data, the literature has documented that price

[13]Since the left hand side variable of the deforestation equation is a transformed variable (inverse hyperbolic sine), quantification of deforested areas include an error term that is not white noise. For this reason, we replicate our maps using the PPML model (Section OA2.4).

[14]Note that this strategy has the drawback to attribute a lot of weight to cells with very small forest cover.

indexes similar to the one we use, e.g based on local crop-specific suitability and world prices, correlate positively and significantly with farmers' income. For instance, McGuirk and Burke (2020) find a negative correlation between a similar price index and farmer's poverty indexes computed from Afrobarometer data. Berman et al. (2021) provide evidence that variations in the international market prices of nutrients or fertilizers are indeed transmitted to local markets in Sub-Saharan Africa. Berman et al. (2020) show a positive correlation with various measures of income from three different datasets: Demographic Health Survey, Afrobarometer and Worldbank Living Standard Measurement Study surveys.

Alternatively, we make use of the data from Porteous (2019), containing information on local prices for 230 markets across 42 countries and four different crops (maize, rice, sorghum and wheat). Our estimates show that the average local prices of crops are clearly correlated with international prices (the unconditional coefficient of correlation ranges from 0.82 to 0.98). Regressing local prices on world prices, controlling for market and crop fixed effects, we find that a one-percent increase in world price is associated with a 0.66 percent increase in local price (Figure OA.16 and Table OA.21). The magnitude of the effect is similar across crops, except for wheat which coefficient is close to 1. Though the data only cover a small part of our tropical sample, this suggests that our main result is indeed partly driven by the response of land managers to local prices.

International demand and trade. Throughout the paper we have interpreted changes in international commodity prices as being demand-driven. The fact that price changes are demand driven alleviates endogeneity problems associated with supply effects, and also has more general implications: this means that influencing demand, including changing individual preferences and consumption behavior, can have a direct impact on deforestation. This interpretation of our results in favor of demand effects is reinforced by the fact that we obtain qualitatively similar results when we consider commodity imports instead of agricultural prices. To do this, we use changes in the aggregate import demand of trading partners as identification variations.

More specifically, we consider a cell c, producing a set of crops k exported by its country i to a set of trading partners j. First, we characterize the importance for country i of export of good k to country j over the period 1990-2000: define $\gamma_{ijk} = \frac{X_{ijk}}{X_{ik}}$ as the share of total exports of country i in good k shipped to country j over the total export of country i in good k. Second, compute the importance of good k for country j: define M_{jkt} as the value of *total* imports of country j in good k during year t. Finally, define α_c^k as the relative suitability of crop k in cell c. With these three components, we can compute our demand index:

$$M_{c,t} = \sum_k \sum_j \alpha_c^k \gamma_{ijk} M_{jkt} \tag{4}$$

Variations in $M_{c,t}$ over time are driven by changes in the total imports of the trading partners of the country in the crops that the cell is suitable at producing. The data to compute trade shares is taken from FAO-Stats. Though this variable is less straightforward to interpret than prices, it is also more directly demand-driven, as its variations solely depends on trade partners' imports of agricultural commodities.

Table 1: Alternative shock: imports in trading partners

	(1)	(2)	(3)	(4)
	Model 1	Model 2	Model 1	Model 2
Estimator	OLS			
ln $M_{c,t}$	0.703^a		0.678^a	
	(0.059)		(0.058)	
× Cover[D1]		-0.208^a		-0.230^a
		(0.071)		(0.071)
× Cover[D2]		0.250^a		0.230^a
		(0.069)		(0.069)
× Cover[D3]		0.377^a		0.359^a
		(0.068)		(0.069)
× Cover[D4]		0.425^a		0.413^a
		(0.068)		(0.068)
× Cover[D5]		0.596^a		0.594^a
		(0.065)		(0.065)
× Cover[D6]		0.621^a		0.614^a
		(0.064)		(0.065)
× Cover[D7]		0.704^a		0.700^a
		(0.064)		(0.064)
× Cover[D8]		0.823^a		0.848^a
		(0.061)		(0.062)
× Cover[D9]		1.008^a		1.038^a
		(0.061)		(0.062)
× Cover[D10]		1.209^a		1.240^a
		(0.063)		(0.064)
ln $M_{c,t}$ × dist. port.			-0.046^a	-0.159^a
			(0.017)	(0.016)
ln $M_{c,t}$ × dist. cap.			0.155^a	0.053^a
			(0.013)	(0.014)
ln $M_{c,t}$ × night lights in 2000			-0.051^a	-0.030^a
			(0.010)	(0.009)
Cell FE	Yes	Yes	Yes	Yes
Country × Year FE	Yes	Yes	Yes	Yes
Observations	166392	166392	166392	166392

Note: Least square estimator. ^{c} significant at 10%; ^{b} significant at 5%; ^{a} significant at 1%. Standard errors clustered by cell in parenthesis. The dependent variable is the hyperbolic inverse sine of the number of pixels deforested in the cell. Cover[x] are bins for deciles of forest cover in 2000. ln dist. port is the log of distance from the closest seaport. ln dist. cap. is the log of the distance from the country's capital city at the beginning of the period. night lights is the average amount of nighttime lights emitted in the cell in 2000.

Our results are qualitatively similar to those obtained with commodity prices (Table 1). Though the effect of price changes and variations in foreign imports cannot be directly compared, we find that the impact of an increase in the trade index on deforestation is substantial: a 10% increase in foreign demand generates a 7% increase in deforestation.

6 Concluding Remarks

Changes in crop prices are found to significantly affect deforestation in the tropics at the local level, thus confirming the key role of market forces (Pendrill et al., 2019). We bring robust statistical evidence that the many agricultural commodities and products traded daily on international markets are responsible for a large share of global deforestation. As the demand for these products increases, new arable land is required. Therefore, the natural solution to arresting deforestation originates on the demand side: if consumers reduce their demand for agricultural products, crop prices will stabilize and deforestation will likely slow. However, forecasts of demand in the coming decades suggest that this is unlikely (Fukase and Martin, 2020). Policies targeting consumers' preferences and behavior should therefore be combined with measures aiming at directly slowing deforestation. Such measures involve multiple actors − corporations, NGOs and governments. Corporations can implement strategies such as supply chain initiatives that promote greater transparency, or they can adopt unilateral or multilateral commitments. However, the complexity of the supply chains, the possibility of leakage, low and selective adoption, and the risk of marginalization of smallholders make the impact of these actions uncertain (Lambin et al., 2018). This was seen, for example, in the case of palm oil supply chains (Lyons-White and Knight, 2018). On the other hand, national and local governments, with the help of NGOs, can implement various policies to reduce deforestation. These include encouraging dietary change, mandating transparency in supply chains, incentivizing companies to adopt effective anti-deforestation strategies, penalizing companies responsible for significant deforestation, and programs to reduce the sensitivity of community incomes to global crop prices. The development of monitoring tools, such as the Transparency for Sustainable Economies initiative[15] and more generally the development of real-time information on areas at risk of deforestation, can facilitate the implementation of anti-deforestation policies (Slough et al., 2021; Moffette et al., 2021b,a).

References

Abman, R. and C. Lundberg (2020). Does free trade increase deforestation? the effects of regional trade agreements. *Journal of the Association of Environmental and Resource Economists 7*(1), 35–72.

Alkama, R. and A. Cescatti (2016). Biophysical climate impacts of recent changes in global forest cover. *Science 351*(6273), 600–604.

Angelsen, A. (1999). Agricultural expansion and deforestation: modelling the impact of population, market forces and property rights. *Journal of Development Economics 58*(1), 185 − 218.

Angelsen, A. (2010). Policies for reduced deforestation and their impact on agricultural production. *Proceedings of the national Academy of Sciences 107*(46), 19639–19644.

[15]The Transparency for Sustainable Economies initiative is an online platform aimed at improving the transparency, clarity and accessibility of information on the commodity supply chains that drive tropical deforestation.

Angelsen, A. and D. Kaimowitz (1999). Rethinking the causes of deforestation: lessons from economic models. *World Bank Research Observer 14*(1), 73–98.

Assunção, J., C. Gandour, and R. Rocha (2015). Deforestation slowdown in the brazilian amazon: prices or policies? *Environment and Development Economics 20*(6), 697–722.

Austin, K. G., A. Schwantes, Y. Gu, and P. S. Kasibhatla (2019). What causes deforestation in Indonesia? *Environmental Research Letters 14*(2), 024007.

Balboni, C., A. Berman, R. Burgess, and B. A. Olken (2022). The economics of tropical deforestation.

Barbier, E. B. and J. C. Burgess (1996). Economic analysis of deforestation in Mexico. *Environment and Development Economics 1*(2), 203–239.

Berman, N., M. Couttenier, and R. Soubeyran (2021). Fertile Ground for Conflict. *Journal of the European Economic Association 19*(1), 82–127.

Berman, N., L. Rotunno, and R. Ziparo (2020). Sweet child of mine: Parental income, child health and inequality.

Bowman, M. S. (2016). Impact of foot-and-mouth disease status on deforestation in brazilian amazon and cerrado municipalities between 2000 and 2010. *Journal of Environmental Economics and Management 75*, 25–40.

Bruederle, A. and R. Hodler (2018). Nighttime lights as a proxy for human development at the local level. *PloS one 13*(9), e0202231.

Buhaug, H. (2006). Local determinants of african civil wars, 1970–2001. *Political Geography 25*(3), 315–335.

Buhaug, H. (2010). Dude, where's my conflict? LSG, relative strenght and the location of civil war. *Conflict Management and Peace Science 27*(2), 107–128.

Burbidge, J. B., L. Magee, and A. L. Robb (1988). Alternative transformations to handle extreme values of the dependent variable. *Journal of the American Statistical Association 83*(401), 123–127.

Busch, J. and K. Ferretti-Gallon (2017). What drives deforestation and what stops it? a meta-analysis. *Review of Environmental Economics and Policy 11*(1), 3–23.

Chaves, L. S. M., J. Fry, A. Malik, A. Geschke, M. A. M. Sallum, and M. Lenzen (2020). Global consumption and international trade in deforestation-associated commodities could influence malaria risk. *Nature communications 11*(1), 1–10.

Chichilnisky, G. (1994). North-south trade and the global environment. *American Economic Review 84*(4), 851–874.

Conley, T. G. (1999). GMM estimation with cross-sectional dependence. *Journal of Econometrics 92*(1), 1–45.

Crippa, M., E. Solazzo, D. Guizzardi, F. Monforti-Ferrario, F. N. Tubiello, and A. Lei (2021). Food systems are responsible for a third of global anthropogenic GHG emissions. *Nature Food*.

Curtis, P. G., C. M. Slay, N. L. Harris, A. Tyukavina, and M. C. Hansen (2018). Classifying drivers of global forest loss. *Science 361*(6407), 1108–1111.

DeFries, R. S., T. Rudel, M. Uriarte, and M. Hansen (2010). Deforestation driven by urban population growth and agricultural trade in the twenty-first century. *Nature Geoscience 3*(3), 178–181.

Doggart, N., T. Morgan-Brown, E. Lyimo, B. Mbilinyi, C. K. Meshack, S. M. Sallu, and D. V. Spracklen (2020). Agriculture is the main driver of deforestation in Tanzania. *Environmental Research Letters 15*(3), 034028.

FAO (2017). The future of food and agriculture: Trends and challenges. Technical report, Food and Agriculture Organization of the United Nations, Rome.

Faria, W. R. and A. Almeida (2016). Relationship between openness to trade and deforestation: Empirical evidence from the Brazilian Amazon. *Ecological Economics 121*(C), 85–97.

Fehlenberg, V., M. Baumann, N. I. Gasparri, M. Piquer-Rodriguez, G. Gavier-Pizarro, and T. Kuemmerle (2017). The role of soybean production as an underlying driver of deforestation in the south american chaco. *Global environmental change 45*, 24–34.

Ferreira, S. (2004). Deforestation, property rights, and international trade. *Land Economics 80*(2), 174–193.

Fischer, G., F. O. Nachtergaele, S. Prieler, E. Teixeira, G. Tóth, H. Van Velthuizen, L. Verelst, and D. Wiberg (2012). Global agro-ecological zones (GAEZ v3. 0)-model documentation.

Foley, J. A., R. DeFries, G. P. Asner, C. Barford, G. Bonan, S. R. Carpenter, F. S. Chapin, M. T. Coe, G. C. Daily, H. K. Gibbs, J. H. Helkowski, T. Holloway, E. A. Howard, C. J. Kucharik, C. Monfreda, J. A. Patz, I. C. Prentice, N. Ramankutty, and P. K. Snyder (2005). Global consequences of land use. *Science 309*(5734), 570–574.

Fukase, E. and W. Martin (2020). Economic growth, convergence, and world food demand and supply. *World Development 132*, 104954.

Gaveau, D. L., M. Linkie, P. Levang, N. Leader-Williams, et al. (2009). Three decades of deforestation in southwest sumatra: effects of coffee prices, law enforcement and rural poverty. *Biological conservation 142*(3), 597–605.

Geist, H. J. and E. F. Lambin (2002, 02). Proximate causes and underlying driving forces of tropical deforestation: Tropical forests are disappearing as the result of many pressures, both local and regional, acting in various combinations in different geographical locations. *BioScience 52*(2), 143–150.

Godar, J., U. M. Persson, E. J. Tizado, and P. Meyfroidt (2015). Towards more accurate and policy relevant footprint analyses: tracing fine-scale socio-environmental impacts of production to consumption. *Ecological Economics 112*, 25–35.

Goldman, E. D., M. Weisse, N. Harris, and M. Schneider (2020). Estimating the role of seven commodities in agriculture-linked deforestation: Oil palm, soy, cattle, wood fiber, cocoa, coffee, and rubber. *World Resources Institute Technical Note*, 1–25.

Goldsmith-Pinkham, P., I. Sorkin, and H. Swift (2020, August). Bartik instruments: What, when, why, and how. *American Economic Review 110*(8), 2586–2624.

Green, J. M., S. A. Croft, A. P. Durán, A. P. Balmford, N. D. Burgess, S. Fick, T. A. Gardner, J. Godar, C. Suavet, M. Virah-Sawmy, et al. (2019). Linking global drivers of agricultural trade to on-the-ground impacts on biodiversity. *Proceedings of the National Academy of Sciences 116*(46), 23202–23208.

Hansen, M. C., P. V. Potapov, R. Moore, M. Hancher, S. A. Turubanova, A. Tyukavina, D. Thau, S. V. Stehman, S. J. Goetz, T. R. Loveland, A. Kommareddy, A. Egorov, L. Chini, C. O. Justice, and J. R. G. Townshend (2013). High-resolution global maps of 21st-century forest cover change. *Science 342*(6160), 850–853.

Hansen, M. C., S. V. Stehman, and P. V. Potapov (2010). Quantification of global gross forest cover loss. *Proceedings of the National Academy of Sciences 107*(19), 8650–8655.

Harding, T., J. Herzberg, and K. Kuralbayeva (2021). Commodity prices and robust environmental regulation: Evidence from deforestation in Brazil. *Journal of Environmental Economics and Management 108*, 102452.

Hargrave, J. and K. Kis-Katos (2013). Economic causes of deforestation in the brazilian amazon: a panel data analysis for the 2000s. *Environmental and Resource Economics 54*(4), 471–494.

Heino, M., M. Kummu, M. Makkonen, M. Mulligan, P. H. Verburg, M. Jalava, and T. A. Räsänen (2015). Forest loss in protected areas and intact forest landscapes: a global analysis. *PloS one 10*(10), e0138918.

Henders, S., U. M. Persson, and T. Kastner (2015). Trading forests: land-use change and carbon emissions embodied in production and exports of forest-risk commodities. *Environmental Research Letters 10*(12), 125012.

Henderson, J. V., A. Storeygard, and D. N. Weil (2012, April). Measuring economic growth from outer space. *American Economic Review 102*(2), 994–1028.

Hendrix, C. S. (2011). Head for the hills? rough terrain, state capacity, and civil war onset. *Civil Wars 13*(4), 345–370.

Hoang, N. T. and K. Kanemoto (2021). Mapping the deforestation footprint of nations reveals growing threat to tropical forests. *Nature Ecology & Evolution*, 1–9.

Hosonuma, N., M. Herold, V. D. Sy, R. S. D. Fries, M. Brockhaus, L. Verchot, A. Angelsen, and E. Romijn (2012, oct). An assessment of deforestation and forest degradation drivers in developing countries. *Environmental Research Letters 7*(4), 044009.

Hsiang, S. M., K. C. Meng, and M. A. Cane (2011). Civil conflicts are associated with the global climate. *Nature 476*(7361), 438–441.

Lambin, E., H. Gibbs, R. Heilmayr, and et al. (2018). The role of supply-chain initiatives in reducing deforestation. *Nature Clim Change 8*, 109–116.

Le Quéré, C., R. M. Andrew, J. G. Canadell, S. Sitch, J. I. Korsbakken, G. P. Peters, A. C. Manning, T. A. Boden, P. P. Tans, R. A. Houghton, R. F. Keeling, S. Alin, O. D. Andrews, P. Anthoni, L. Barbero, L. Bopp, F. Chevallier, L. P. Chini, P. Ciais, K. Currie, C. Delire, S. C. Doney, P. Friedlingstein, T. Gkritzalis, I. Harris, J. Hauck, V. Haverd, M. Hoppema, K. Klein Goldewijk, A. K. Jain, E. Kato, A. Körtzinger, P. Landschützer, N. Lefèvre, A. Lenton, S. Lienert, D. Lombardozzi, J. R. Melton, N. Metzl, F. Millero, P. M. S. Monteiro, D. R. Munro, J. E. M. S. Nabel, S. Nakaoka, K. O'Brien, A. Olsen, A. M. Omar, T. Ono, D. Pierrot, B. Poulter, C. Rödenbeck, J. Salisbury, U. Schuster, J. Schwinger, R. Séférian, I. Skjelvan, B. D. Stocker, A. J. Sutton, T. Takahashi, H. Tian, B. Tilbrook, I. T. van der Laan-Luijkx, G. R. van der Werf, N. Viovy, A. P. Walker, A. J. Wiltshire, and S. Zaehle (2016). Global carbon budget 2016. *Earth System Science Data 8*(2), 605–649.

Leblois, A., O. Damette, and J. Wolfersberger (2017). What has driven deforestation in developing countries since the 2000s? evidence from new remote-sensing data. *World Development 92*(C), 82–102.

Lundberg, C. and R. Abman (2021). Maize price volatility and deforestation. *American Journal of Agricultural Economics*.

Lyons-White, J. and A. T. Knight (2018). Palm oil supply chain complexity impedes implementation of corporate no-deforestation commitments. *Global Environmental Change 50*, 303–313.

MacKinnon, J. G. and L. Magee (1990). Transforming the dependent variable in regression models. *International Economic Review 31*(2), 315–339.

Matricardi, E. A. T., D. L. Skole, O. B. Costa, M. A. Pedlowski, J. H. Samek, and E. P. Miguel (2020). Long-term forest degradation surpasses deforestation in the brazilian amazon. *Science 369*(6509), 1378–1382.

McGuirk, E. and M. Burke (2020). The Economic Origins of Conflict in Africa. *Journal of Political Economy 128*(10), 3940–3997.

Michalopoulos, S. and E. Papaioannou (2014). National institutions and subnational development in Africa. *Quarterly Journal of Economics 129*(1), 151–213.

Moffette, F., J. Alix-Garcia, K. Shea, and A. H. Pickens (2021a). Freely available deforestation alerts can reduce emissions from land-use change. *Nature Climate Change 11*(11), 913–914.

Moffette, F., J. Alix-Garcia, K. Shea, and A. H. Pickens (2021b). The impact of near-real-time deforestation alerts across the tropics. *Nature Climate Change 11*(2), 172–178.

Ordway, E. M., G. P. Asner, and E. F. Lambin (2017). Deforestation risk due to commodity crop expansion in sub-Saharan Africa. *Environmental Research Letters 12*(4), 044015.

Ordway, E. M., R. L. Naylor, R. N. Nkongho, and E. F. Lambin (2017). Oil palm expansion in Cameroon: Insights into sustainability opportunities and challenges in Africa. *Global Environmental Change 47*, 190–200.

Ordway, E. M., R. L. Naylor, R. N. Nkongho, and E. F. Lambin (2019). Oil palm expansion and deforestation in southwest Cameroon associated with proliferation of informal mills. *Nature communications 10*(1), 1–11.

Pence, K. M. (2006). The role of wealth transformations: An application to estimating the effect of tax incentives on saving. *B.E. Journal of Economic Analysis & Policy 5*(1).

Pendrill, F., T. A. Gardner, P. Meyfroidt, U. M. Persson, J. Adams, T. Azevedo, M. G. Bastos Lima, M. Baumann, P. G. Curtis, V. De Sy, et al. (2022). Disentangling the numbers behind agriculture-driven tropical deforestation. *Science 377*(6611), eabm9267.

Pendrill, F., U. M. Persson, J. Godar, and T. Kastner (2019). Deforestation displaced: trade in forest-risk commodities and the prospects for a global forest transition. *Environmental Research Letters 14*(5), 055003.

Pendrill, F., U. M. Persson, J. Godar, T. Kastner, D. Moran, S. Schmidt, and R. Wood (2019). Agricultural and forestry trade drives large share of tropical deforestation emissions. *Global Environmental Change 56*, 1–10.

Porteous, O. (2019). High trade costs and their consequences: An estimated dynamic model of african agricultural storage and trade. *American Economic Journal: Applied Economics 11*(4), 327–66.

Potapov, P., M. C. Hansen, S. V. Stehman, T. R. Loveland, and K. Pittman (2008). Combining modis and landsat imagery to estimate and map boreal forest cover loss. *Remote sensing of environment 112*(9), 3708–3719.

Probst, B., A. BenYishay, A. Kontoleon, and T. N. dos Reis (2020). Impacts of a large-scale titling initiative on deforestation in the Brazilian Amazon. *Nature Sustainability 3*(12), 1019–1026.

Rudel, T. K., L. Schneider, M. Uriarte, B. L. Turner, R. DeFries, D. Lawrence, J. Geoghegan, S. Hecht, A. Ickowitz, E. F. Lambin, et al. (2009). Agricultural intensification and changes in cultivated areas, 1970-2005. *Proceedings of the National Academy of Sciences 106*(49), 20675–20680.

Sandler, T. (1993). Tropical deforestation: Markets and market failures. *Land Economics 69*(3), 225–233.

Slough, T., J. Kopas, and J. Urpelainen (2021). Satellite-based deforestation alerts with training and incentives for patrolling facilitate community monitoring in the peruvian amazon. *Proceedings of the National Academy of Sciences 118*(29).

Song, X.-P., M. C. Hansen, S. V. Stehman, P. V. Potapov, A. Tyukavina, E. F. Vermote, and J. R. Townshend (2018). Global land change from 1982 to 2016. *Nature 560*, 639–643.

Souza-Rodrigues, E. (2019). Deforestation in the Amazon: A unified framework for estimation and policy analysis. *Review of Economic Studies 86*(6), 2713–2744.

Tollefson, J. (2020). Why deforestation and extinctions make pandemics more likely. *Nature 584*(7820), 175–177.

Turner, B. L., E. F. Lambin, and A. Reenberg (2007). The emergence of land change science for global environmental change and sustainability. *Proceedings of the National Academy of Sciences 104*(52), 20666–20671.

Vancutsem, C., F. Achard, J.-F. Pekel, G. Vieilledent, S. Carboni, D. Simonetti, J. Gallego, L. Aragão, and R. Nasi (2021). Long-term (1990-2019) monitoring of forest cover changes in the humid tropics. *Science Advances 7*(10), eabe1603.

Wheeler, D., D. Hammer, R. Kraft, S. Dasgupta, and B. Blankespoor (2013). Economic dynamics and forest clearing: A spatial econometric analysis for indonesia. *Ecological Economics 85*, 85–96.

World Bank Group (2020). Commodity markets outlook, october 2020. https://openknowledge.worldbank.org/handle/10986/34621 , License: CC BY 3.0 IGO.

Wren-Lewis, L., L. Becerra-Valbuena, and K. Houngbedji (2020). Formalizing land rights can reduce forest loss: Experimental evidence from Benin. *Science Advances 6*(26), eabb6914.

Online Appendix – Not for publication

OA1 Data and descriptive statistics

OA1.1 Tree cover and deforestation

Information on tree cover for the year 2000 is available at a resolution of 1 arc-second (around 30m$\times$30m). The tree cover is defined by Hansen et al. (2013) as canopy closure for all vegetation taller than 5m in height. We consider two thresholds to consider a pixel as a forest: a canopy cover threshold of 25 and 50% of a pixel in year 2000. The main results define forest pixel as having at least 25% of forest cover, while robustness checks were run for a threshold of 50% (Section OA2.6). Hansen et al. (2013) estimate tree cover loss annually over the 2001-2018 period (version 1.6), defined as a stand-replacement disturbance, or a change from a forest to non-forest state. The data provides a year of tree cover loss for every pixel with more than 1% of forest cover (vegetation taller than 5m height) in 2000 that is estimated to endure a loss of more than 50% of the 2000 forest cover between 2001 and 2018. We consider that the whole pixel (30x30m) tree cover was reduced to zero when losses occur. Forest degradation, for example selective removals from within forested stands that do not lead to a non-forest state, was not included in the change characterization. Moreover, the data does not allow to distinguish quality of the canopy and select every vegetation higher than 5m, potentially leading to consider secondary forest loss as deforestation.

OA1.2 Suitability

A crucial information to define our cell-specific price crop index is the crop-specific agronomic suitability of a cell. The FAO provides for the suitability for 45 crops at a resolution of 5 arc minute (FAO's global agroecological zones, GAEZ). These data are constructed from models that use location characteristics, such as climate information (rainfall and temperature, for instance) and soil characteristics. This information is then combined with crops' characteristics (in terms of growing requirements) to generate a global GIS raster of the suitability for each of the 45 crops. Constrained by the availability of international price data, our final sample encompasses 15 crops.

OA1.3 Other data

Throughout the manuscript we make use of different datasets. First, we use information on night-time lights in 2000 aiming to approximate local economic development.[16] Second, we compute the geodesic distances between each centroid grid cell of 0.5$\times$0.5 degree longitude and latitude and the closest port. We use location of ports from *World Port Index* dataset[17] that provides GPS location of ports with a depth larger than 11 meters. Third, we compute the geodesic distance between each centroid grid cells and the

[16]Data from the DMSP-OLS, Nighttime Lights Time Series Version 4 (Average Visible, Stable Lights, & Cloud Free Coverages), as available in PRIO-GRID.

[17]Available at the following link https://msi.nga.mil/Publications/WPI

capital city of each country.[18] Fourth, to compute the crop-specific country market share in world trade, we make use of the dataset on exports and imports from the FAO.[19]. Last, we make use of information on rainfall and temperature from the climate research unit from the University of East Anglia.[20]

OA1.4 Forest cover and deforestation: maps and descriptive statistics

Figure OA.1: Cumulated deforestation, 2001-2018

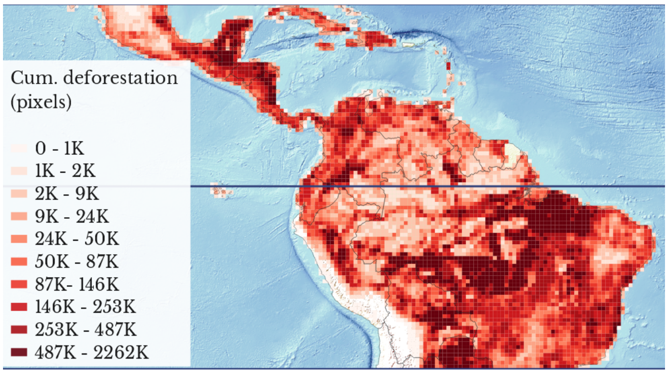

(a) Americas

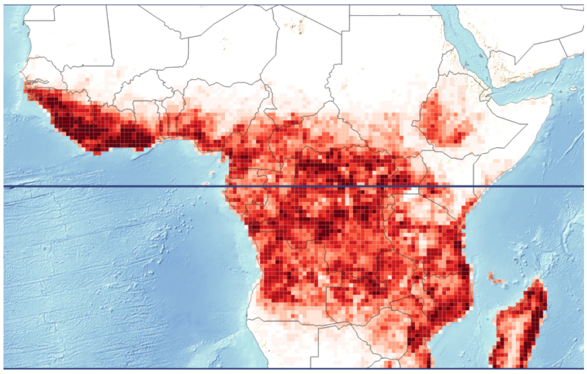

(b) Africa

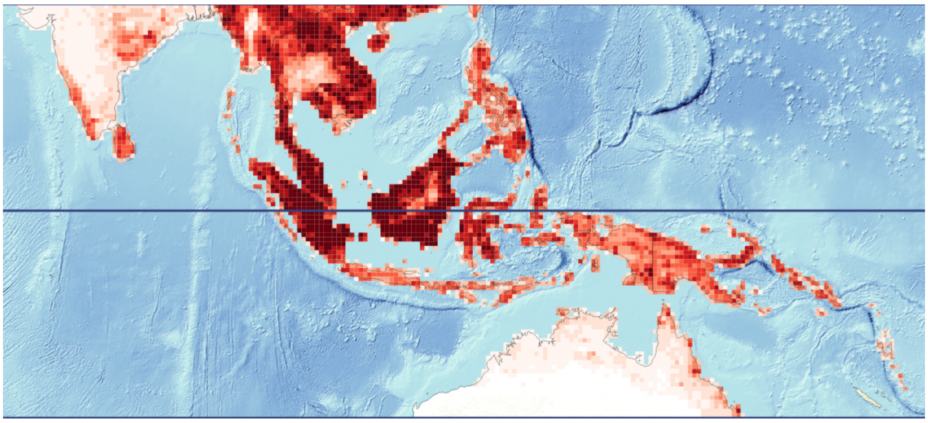

(c) Asia and Oceania

Note: Accumulated deforestation, in number of pixels (max. total of land pixel in a cell is 4000K), forest defined with a 25% threshold. Source: Hansen et al. (2013).

[18]We use the distance to the capital city at the beginning of the period, as in a very small number of cases the capital city has changed during the period.

[19]Faostat data site http://www.fao.org/faostat/en

[20]Available at https://crudata.uea.ac.uk/cru/data/hrg/

Figure OA.2: Forest cover in 2000

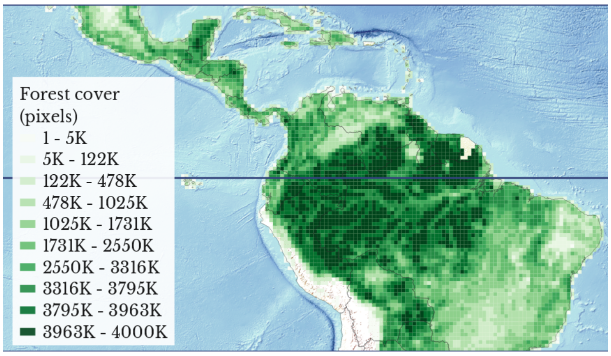

(a) Americas

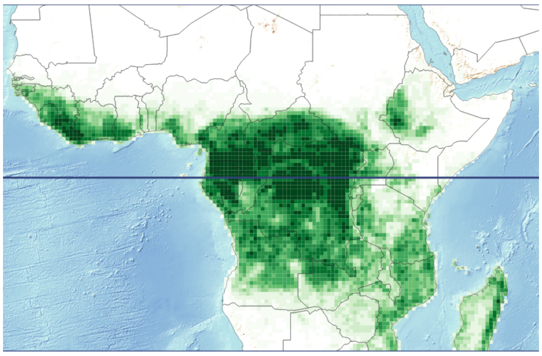

(b) Africa

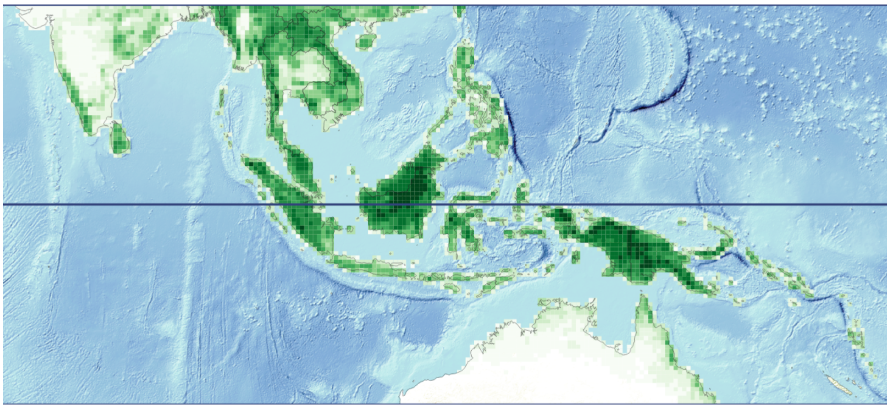

(c) Asia and Oceania

Note: Number of pixels covered by forest, using a 25% canopy cover threshold. Year: 2000. The maximum total of land pixels per cell is 4000K.

Figure OA.3: Percentage of deforested pixels by cell cover decile

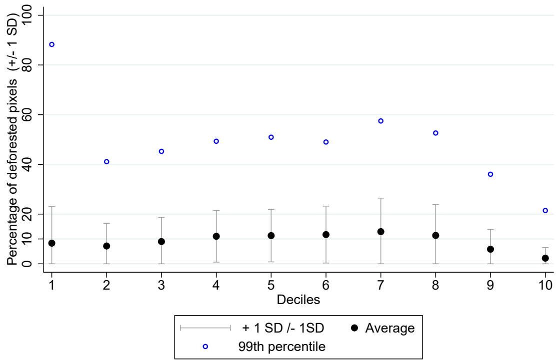

Source: The figure represents the number of deforested pixels over the total number of pixels in the cell at the beginning of the period, by groups of cells defined based on deciles of initial forest cover. Authors' computation from Hansen et al. (2013), using a canopy threshold of 25%.

Table OA.1: Suitability within-country variance

Crop	Within Country share	Crop	Within Country share	Crop	Within Country share
Banana	0.61	Cotton	0.58	Sugar	0.69
Barley	0.64	Maize	0.62	Soybean	0.57
Cocoa	0.64	Oil Palm	0.66	Tea	0.70
Coconut	0.74	Rice	0.71	Tobacco	0.50
Coffee	0.64	Sorghum	0.51	Wheat	0.63

Source: Authors' computation from GAEZ data. Share of variance of average cell suitability within country in total variance.

OA1.5 International prices: descriptive statistics

Figure OA.4: Average price index variation, 2001-2018

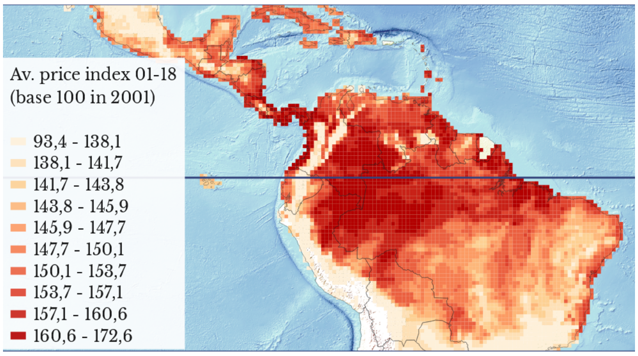

(a) Americas

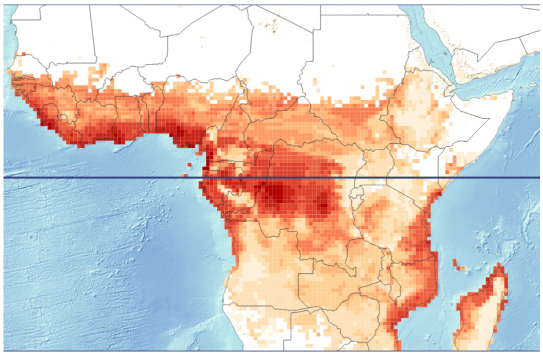

(b) Africa

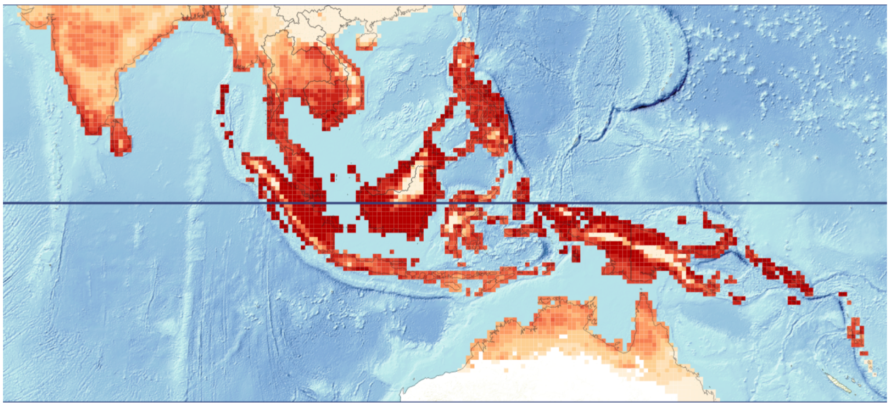

(c) Asia and Oceania

Note: Average value of the crop price index over the 2001-2018 period, taking 2001 as a base year.

Figure OA.5: Crop price series

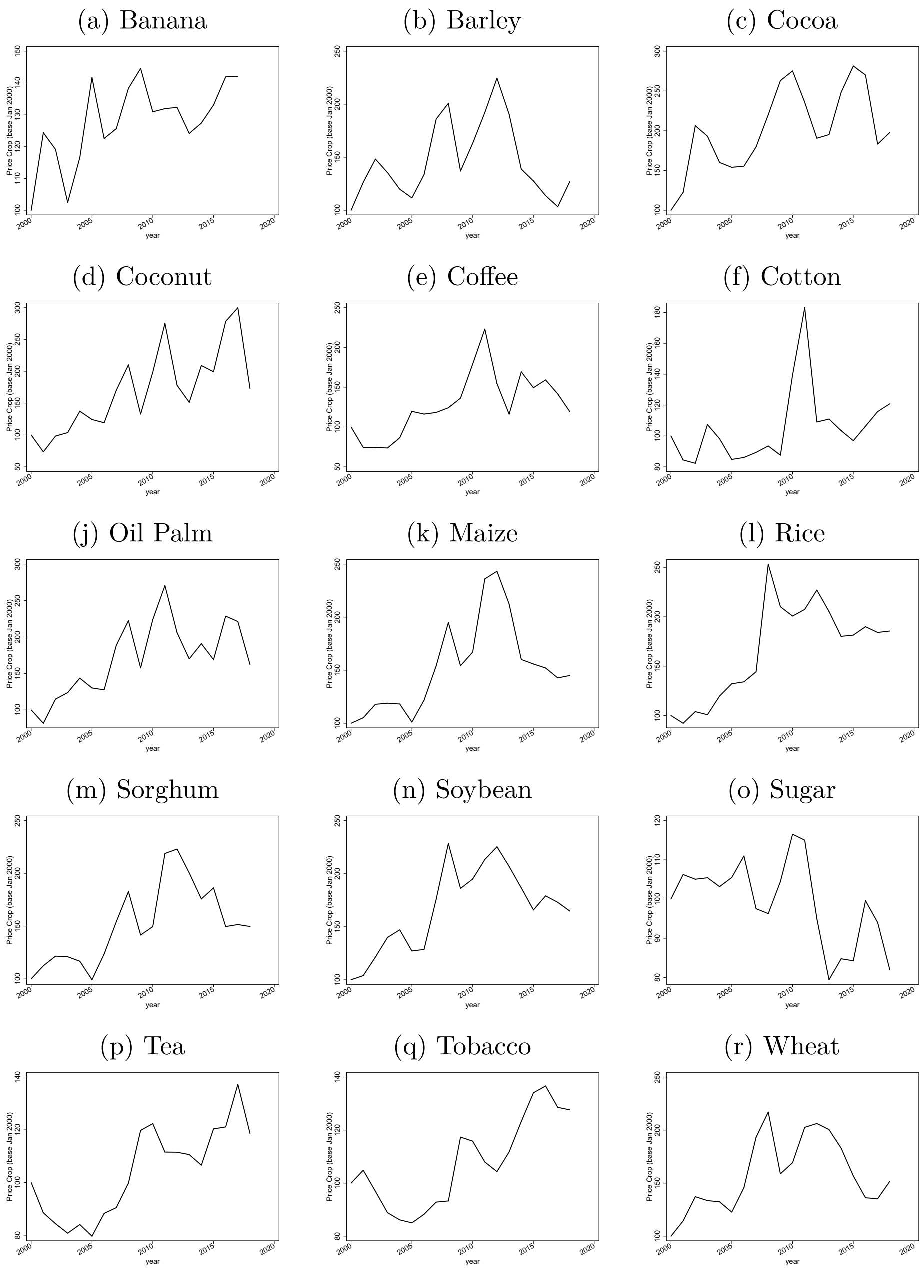

Source: World Bank.

Table OA.2: Crop prices correlation matrix

	banana	barley	cocoa	coconut	coffee	cotton	maize	oilpalm	rice	sorghum	soybean	sugar	tea	tobacco	wheat
banana	1														
barley	0.137	1													
cocoa	0.528	0.231	1												
coconut	0.592	0.154	0.569	1											
coffee	0.552	0.329	0.633	0.783	1										
cotton	0.0802	0.304	0.336	0.593	0.720	1									
maize	0.371	0.839	0.470	0.549	0.677	0.583	1								
oilpalm	0.576	0.485	0.639	0.914	0.852	0.679	0.767	1							
rice	0.681	0.574	0.641	0.676	0.708	0.413	0.831	0.813	1						
sorghum	0.373	0.754	0.526	0.602	0.682	0.536	0.960	0.748	0.804	1					
soybean	0.533	0.736	0.627	0.663	0.684	0.487	0.916	0.861	0.935	0.878	1				
sugar	-0.0820	-0.0348	-0.107	-0.166	0.0465	0.182	-0.205	-0.0425	-0.293	-0.371	-0.249	1			
tea	0.550	0.0283	0.572	0.731	0.652	0.465	0.475	0.640	0.690	0.525	0.552	-0.332	1		
tobacco	0.474	-0.185	0.615	0.612	0.512	0.297	0.257	0.433	0.464	0.389	0.325	-0.469	0.874	1	
wheat	0.345	0.900	0.465	0.427	0.542	0.368	0.894	0.691	0.782	0.870	0.900	-0.241	0.262	0.0693	1

Source: World Bank and authors' computation.

OA1.6 Summary statistics

Table OA.3 displays the summary statistics of all variables used in the paper.

Table OA.3: Summary statistics

Variable	Mean	Std. Dev.	Min.	Max.	N
Forest cover in 2000 (forest: > =25%)	2160762.943	1468356.427	5002	4000000	221184
Forest cover in 2000 (forest: > =50%)	1733182.742	1517453.892	0	4000000	221184
Deforestation (pixel share, forest: > =25%)	0.005	0.01	0	0.43	221184
Deforestation (pixel share, forest: > =50%)	0.008	0.023	0	1	220122
Deforestation (pixel count, forest: > =25%)	10553.688	22859.436	0	749160	221184
Deforestation (pixel count, forest: > =50%)	9074.951	21442.323	0	746363	221184
Inverse hyperbolic sine transformation of Deforestation (pixel count, forest: > =25%)	8.028	2.688	0	14.22	221184
Inverse hyperbolic sine transformation of Deforestation (pixel count, forest: > =50%)	7.417	3.141	0	14.216	221184
Price index	66.763	21.041	1.547	215.39	221184
Distance to nearest seaport in km (dist. port)	604.582	436.82	1.811	1893.287	221184
Distance to capital city in km (dist. cap.)	901.101	793.15	1.773	7916.136	221184
Stable night-time lights in 2000 (night lights)	0.842	2.594	0	44.547	221184

Note: See appendix Sections OA1.1, OA1.2 and OA1.3 for more details.

OA2 Statistical analysis

OA2.1 Baseline estimates

This sub-section contains the two Tables related to the Figures displaying the baseline estimates in the manuscript. Table OA.4 displays the estimates used to construct Figure 1, Model 1 (Column 1) and Model 2 (Column 2). Table OA.5 shows the estimates used in Figure 3. Column (1) provides the estimates of Model 1, that is of specification (3) when we include interaction variables between the price index and cell characteristics (distance to the closest port, distance to the capital city and the intensity of nighttime lights in 2000). In column (2), we provide the estimates of the same specification, but with the price index interacted with a binary variable for each decile of the initial forest cover distribution. Finally, in column (3) we control for a full set of interactions between country dummies and the price index.

Table OA.4: Baseline results

Model	(1) Model 1	(2) Model 2
ln Price	1.267^{a}	
	(0.088)	
× Cover[D1]		-0.136
		(0.113)
× Cover[D2]		0.566^{a}
		(0.104)
× Cover[D3]		0.866^{a}
		(0.102)
× Cover[D4]		0.877^{a}
		(0.101)
× Cover[D5]		1.115^{a}
		(0.097)
× Cover[D6]		1.177^{a}
		(0.097)
× Cover[D7]		1.409^{a}
		(0.098)
× Cover[D8]		1.594^{a}
		(0.094)
× Cover[D9]		1.837^{a}
		(0.092)
× Cover[D10]		2.153^{a}
		(0.095)
Cell FE	Yes	Yes
Country × Year FE	Yes	Yes
Observations	221184	221184
Period	2001-2018	2001-2018
R^2	0.860	0.861

Note: Least square estimator. ^{c} significant at 10%; ^{b} significant at 5%; ^{a} significant at 1%. Standard errors clustered at the cell level in parentheses. The dependent variable is the hyperbolic inverse sine of the number of pixels deforested in the cell. ln Price is our crop price index, defined in equation (2). Cover[x] are bins for deciles of forest cover in 2000.

Table OA.5: Baseline results with cell characteristics

	(1) Model 1	(2) Model 2	Model 3
ln Price	1.166^{a}		
	(0.087)		
× ln dist. port	-0.111^{a}	-0.287^{a}	-0.125^{a}
	(0.025)	(0.024)	(0.026)
× ln dist. cap.	0.189^{a}	0.032	0.177^{a}
	(0.024)	(0.025)	(0.025)
× night lights in 2000	-0.101^{a}	-0.060^{a}	-0.110^{a}
	(0.015)	(0.014)	(0.016)
× Cover[D1]		-0.189^{c}	
		(0.113)	
× Cover[D2]		0.512^{a}	
		(0.103)	
× Cover[D3]		0.809^{a}	
		(0.101)	
× Cover[D4]		0.826^{a}	
		(0.100)	
× Cover[D5]		1.077^{a}	
		(0.097)	
× Cover[D6]		1.132^{a}	
		(0.097)	
× Cover[D7]		1.373^{a}	
		(0.097)	
× Cover[D8]		1.625^{a}	
		(0.095)	
× Cover[D9]		1.909^{a}	
		(0.094)	
× Cover[D10]		2.258^{a}	
		(0.098)	
Cell FE	Yes	Yes	Yes
Country × Year FE	Yes	Yes	Yes
Country FE × price	No	No	Yes
Observations	221184	221184	221184
Period	2001-2018	2001-2018	2001-2018

Note: Least square estimator. ^{c} significant at 10%; ^{b} significant at 5%; ^{a} significant at 1%. Standard errors clustered at the cell level in parentheses. The dependent variable is the hyperbolic inverse sine of the number of pixels deforested in the cell. ln Price is our crop price index, defined in equation (2). Cover[x] are bins for deciles of forest cover in 2000. ln dist. port is the log of distance from the closest seaport. ln dist. cap. is the log of the distance from the country's capital city at the beginning of the period. night lights is the average amount of nighttime lights emitted in the cell in 2000.

OA2.2 Focus on the Congo Basin (grey scale)

Figure OA.6: Focus on the Congo Basin: (b) Additional contribution of cell-level characteristics (grey scale)

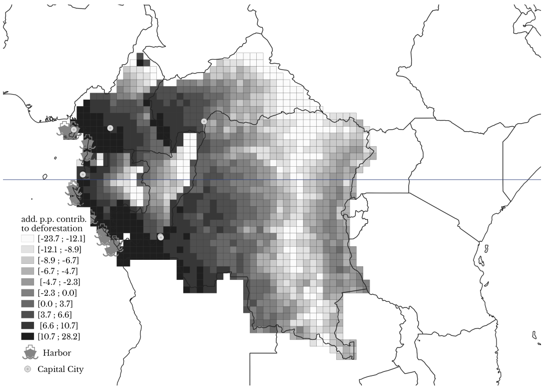

Note: Quantification is based on the estimation results of Model 2 (see Section 3). We first compute the predicted level of deforestation using observed prices (the benchmark). We then compute a counterfactual level of deforestation assuming fixed prices at their 2001 level. Finally, we sum these predictions by cell over the period and compute for each cell the contribution of prices as the difference between the benchmark and the counterfactual prediction, divided by the counterfactual. The Figure shows the difference in p.p. between Figure (4.a) and the sample quantification based on a specification where interaction terms between prices and cell characteristics are included (dist. port, dist cap. and light lights in 2000).

OA2.3 Full quantification with cell-level characteristics

Figure OA.7 provides the same quantification as in Figure 4, but over all the Tropics.

Figure OA.7: Additional contrib. of cell-level characteristics, full Tropics sample

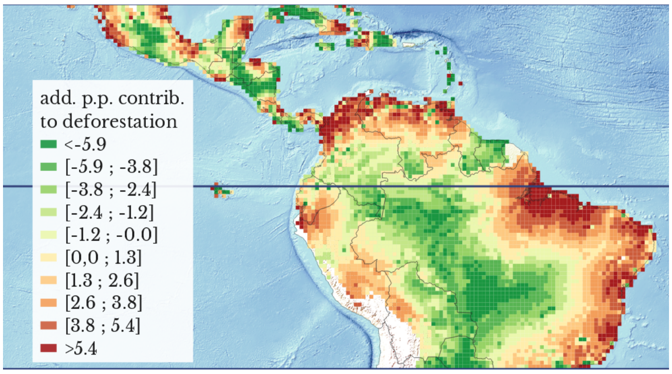

(a) Americas

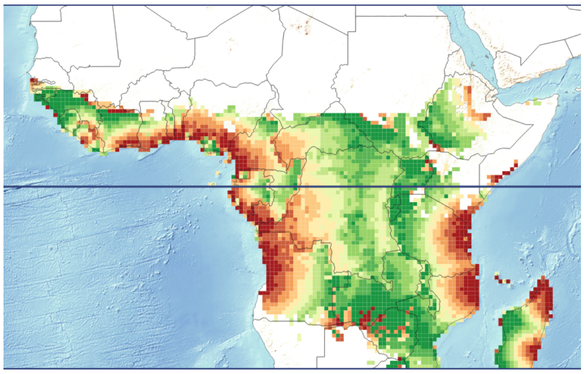

(b) Africa

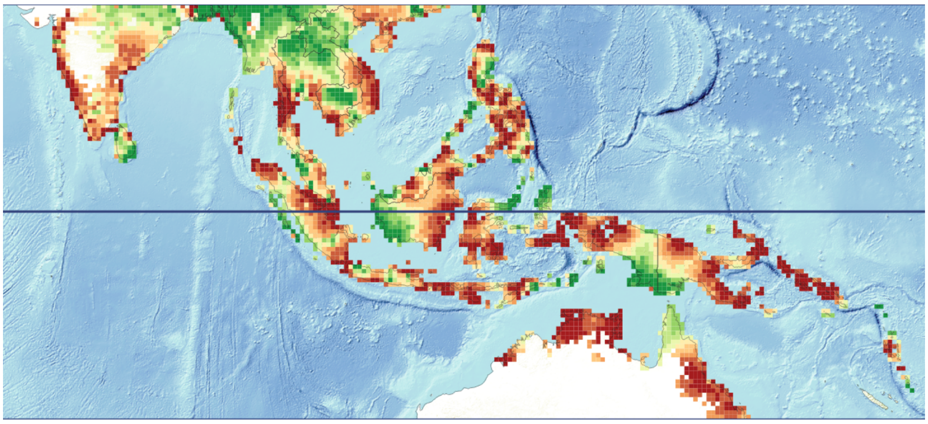

(c) Asia and Oceania

Note: Difference (in percentage point) in the contribution of crop prices to deforestation when interacting variables with cell characteristics (Model 2, Figure 3), compared to our baseline (Figure 2). For each model, the quantification is computed in the following way. First, we compute the predicted level of deforestation using observed prices, our benchmark). Then, we compute a counterfactual level of deforestation assuming fixing prices at their 2001 level. Finally, we sum these predictions by cell over the period, and compute for each cell the contribution of prices as the difference between the benchmark and the counterfactual predictions, divided by the counterfactual.

OA2.4 Quantifications, PPML estimator

Figures OA.8 to OA.11 provides the equivalent to Figures 2, 4, OA.6 and OA.7, using a PPML estimator instead of OLS with an Inverse Hyperbolic Sine transformation.

Figure OA.8: Contribution of crop prices increases to deforestation, 2001-2018, PPML

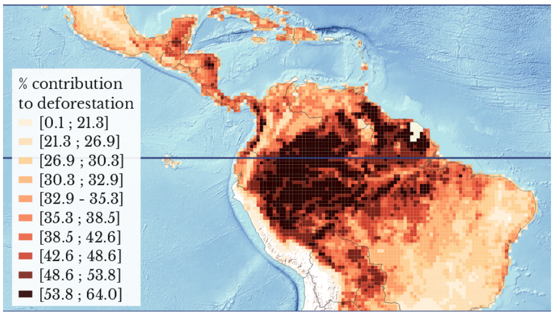

(a) Americas

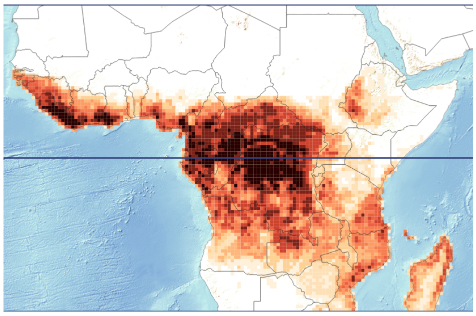

(b) Africa

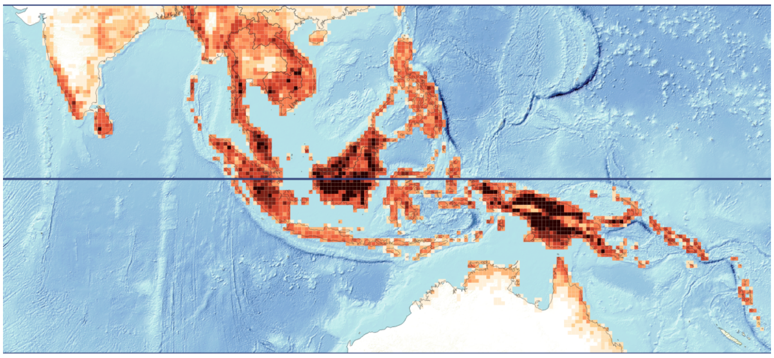

(c) Asia and Oceania

Note: Contribution of crop price increases to deforestation. Quantification based on the estimation results of Model 2 (see Section 3), using a PPML estimator instead of OLS. We first compute the predicted level of deforestation using observed prices, our benchmark). Then we compute a counterfactual level of deforestation assuming fixing prices at their 2001 level. Finally, we sum these predictions by cell over the period, and compute for each cell the contribution of prices as the difference between the benchmark and the counterfactual predictions, divided by the counterfactual.

Figure OA.9: Focus on the Congo Basin, PPML estimator

(a) Baseline quantification

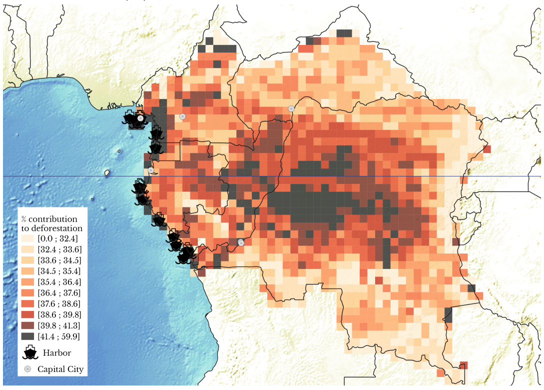

(b) Additional contribution of cell-level characteristics

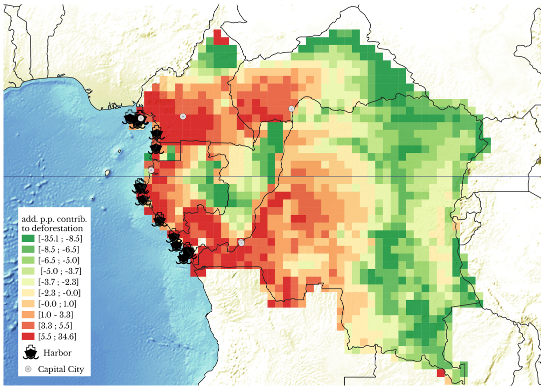

Note: Figure (a) shows the contribution of crop price increases to forest loss, sample restricted to the Congo Basin. Quantification based on the estimation results of Model 2 (see Section 3), estimated with a PPML estimator instead of OLS. We first compute the predicted level of deforestation using observed prices, our benchmark. Then we compute a counterfactual level of deforestation assuming fixing prices at their 2001 level. Finally, we sum these predictions by cell over the period, and compute for each cell the contribution of prices as the difference between the benchmark and the counterfactual predictions, divided by the counterfactual. Figure (b) shows the difference in p.p. between Figure (a) and the sample quantification based on a specification where interaction terms between prices and cell characteristics are included, again using a PPML estimator.

Figure OA.10: Focus on the Congo Basin, PPML estimator: (b) Additional contribution of cell-level characteristics (grey scale)

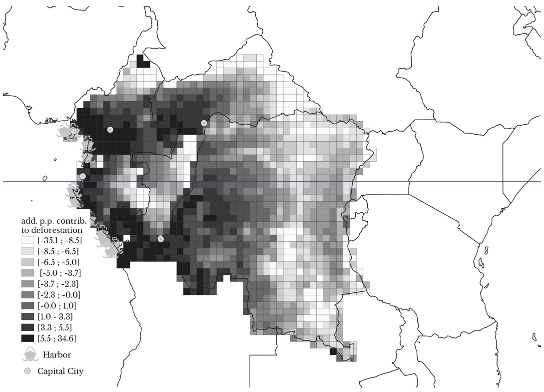

Note: Quantification based on the estimation results of Model 2 (see Section 3), estimated with a PPML estimator instead of OLS. We first compute the predicted level of deforestation using observed prices, our benchmark. Then we compute a counterfactual level of deforestation assuming fixing prices at their 2001 level. Finally, we sum these predictions by cell over the period, and compute for each cell the contribution of prices as the difference between the benchmark and the counterfactual predictions, divided by the counterfactual. The Figure shows the difference in p.p. between Figure (OA.9.a) and the sample quantification based on a specification where interaction terms between prices and cell characteristics are included, again using a PPML estimator.

Figure OA.11: Additional contrib. of cell-level characteristics, full Tropics sample, PPML

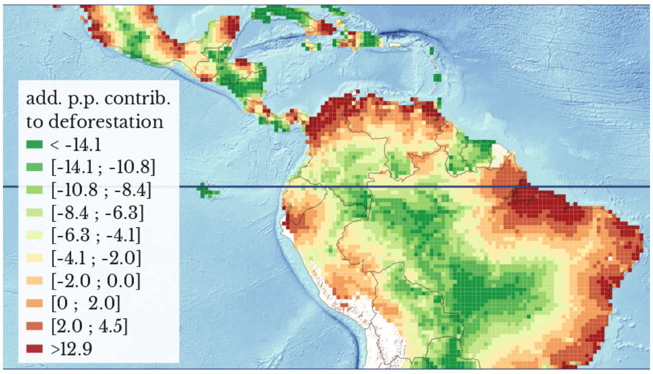

(a) Americas

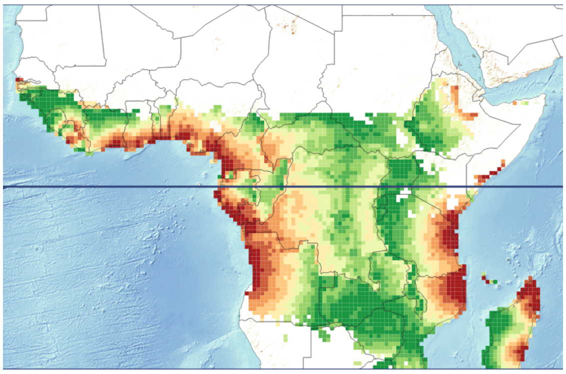

(b) Africa

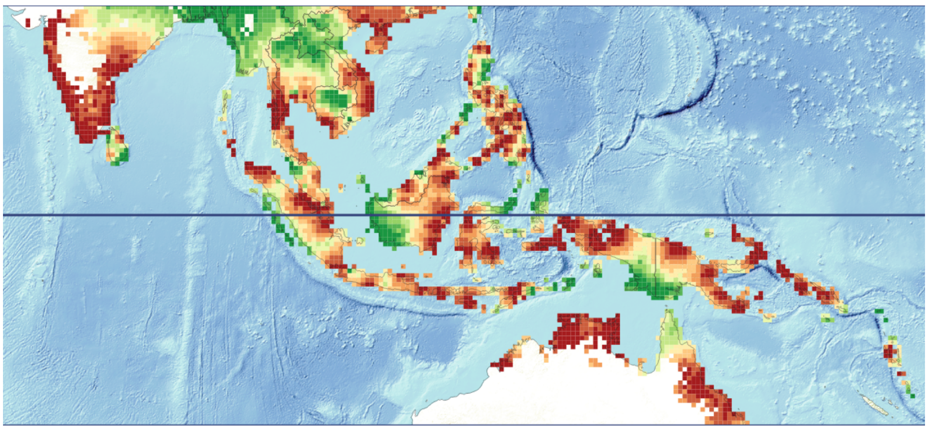

(c) Asia and Oceania

Note: Difference (in percentage point) in the contribution of crop prices to deforestation when interacting variables with cell characteristics (Model 2, Figure 3), compared to our baseline (Figure OA.8); these maps use a PPML estimator instead of OLS. For each model, the quantification is computed in the following way. First, we compute the predicted level of deforestation using observed prices, our benchmark). Then, we compute a counterfactual level of deforestation assuming fixing prices at their 2001 level. Finally, we sum these predictions by cell over the period, and compute for each cell the contribution of prices as the difference between the benchmark and the counterfactual predictions, divided by the counterfactual.

OA2.5 Country characteristics

In this section, we use data from the Worldwide Governance Indicators (WBGI) as well as information on GDP per capita and a global measure of institutional quality, the International Country Risk Guide (ICRG) index. We use the value of these variables at the beginning of the period, in 2000, interacted with our price index. We control for continent fixed effects and forest cover, both interacted with our price index.

Table OA.6 displays the results. Several observations can be made. First, though the significance of the effect of distance to capital city varies, the coefficients of cell specific characteristics (distance to port, nighttime luminosity) are quite stable. Second, the significance of the estimates of the country-level institutions variables vary. A high institutional quality (ICRG index) limits the impact of international crop prices on deforestation (columns 1 and 2); GDP per capita does not seem to play a role (columns 2 and 4). In column 4, where all the variables are included, we find that the effect of crop prices is lower in countries with better control of corruption, rule of law and to a lesser extent regulatory quality, but worsens in countries where government effectiveness and accountability are high. Though these are interesting results, interpreting them would require thinking theoretically about how different types of institutions should affect the response of deforestation to crop price variations. Such a theoretical study is beyond the scope of the paper, which is why we chose, in our main results, to control for country characteristics through fixed effects (interacted with prices) rather than directly investigating the impact of country characteristics.

Table OA.6: Baseline results with country characteristics

	(1)	(2)	(3)	(4)
ln Price				
× ln dist. port	-0.269^a	-0.269^a	-0.289^a	-0.289^a
	(0.025)	(0.025)	(0.025)	(0.025)
× ln dist. cap.	0.045^c	0.042	0.020	0.021
	(0.025)	(0.025)	(0.026)	(0.026)
× night lights in 2000	-0.064^a	-0.064^a	-0.070^a	-0.069^a
	(0.014)	(0.014)	(0.015)	(0.015)
× ICRG Index	-4.611^a	-5.477^a		
	(1.222)	(1.328)		
× ln real GDP per cap.		0.327		-0.201
		(0.208)		(0.242)
× Control of corruption (WBGI)			-1.600^b	-1.614^b
			(0.758)	(0.756)
× Voice and accountability (WBGI)			1.928^a	1.948^a
			(0.467)	(0.465)
× Government effectiveness (WBGI)			3.716^a	4.010^a
			(1.072)	(1.067)
× Regulatory Quality (WBGI)			-0.581	-0.731
			(0.598)	(0.596)
× Political Stability (WBGI)			0.795^a	0.758^a
			(0.259)	(0.259)
× Rule of Law (WBGI)			-3.072^a	-2.991^a
			(0.846)	(0.850)
Cell FE	Yes	Yes	Yes	Yes
Country × Year FE	Yes	Yes	Yes	Yes
Region FE × ln Price	Yes	Yes	Yes	Yes
Forest cover × ln Price	Yes	Yes	Yes	Yes
Observations	208476	208476	214326	214326

Note: Least square estimator. ^{c} significant at 10%; ^{b} significant at 5%; ^{a} significant at 1%. Standard errors clustered at the cell level in parentheses. The dependent variable is the hyperbolic inverse sine of the number of pixels deforested in the cell. ln Price is our crop price index, defined in equation (2). Forest cover × ln Price is a set of interaction variables, Cover[x] × ln Price, where Cover[x] are bins for deciles of forest cover in 2000. ln dist. port is the log of distance from the closest seaport. ln dist. cap. is the log of the distance from the country's capital city at the beginning of the period. night lights is the average amount of nighttime lights emitted in the cell in 2000. All the country level variables are taken at the beginning of the period, in 2000.

OA2.6 Sensitivity analysis

OA2.6.1 Canopy threshold & PPML

Table OA.7: Sensitivity analysis of baseline estimates: canopy threshold & PPML

	(1)	(2)	(3)	(4)
Model	Model 1	Model 2	Model 1	Model 2
Canopy threshold	50%	50%	25%	25%
Estimator	OLS	OLS	PPML	PPML
ln Price	1.351^a		1.377^a	
	(0.088)		(0.117)	
× Cover[D1]		0.080		0.375^b
		(0.113)		(0.167)
× Cover[D2]		0.451^a		0.881^a
		(0.108)		(0.149)
× Cover[D3]		0.761^a		0.877^a
		(0.105)		(0.132)
× Cover[D4]		0.813^a		1.085^a
		(0.104)		(0.134)
× Cover[D5]		1.109^a		1.141^a
		(0.100)		(0.132)
× Cover[D6]		1.193^a		1.093^a
		(0.099)		(0.129)
× Cover[D7]		1.531^a		1.267^a
		(0.099)		(0.126)
× Cover[D8]		1.739^a		1.557^a
		(0.095)		(0.126)
× Cover[D9]		1.990^a		1.768^a
		(0.093)		(0.126)
× Cover[D10]		2.297^a		1.886^a
		(0.096)		(0.148)
Cell FE	Yes	Yes	Yes	Yes
Country × Year FE	Yes	Yes	Yes	Yes
Observations	220122	220122	221006	221006

Note: Least square estimator in columns (1) and (2), PPML in columns (3) and (4). ^{c} significant at 10%; ^{b} significant at 5%; ^{a} significant at 1%. Standard errors clustered at the cell level in parentheses. The dependent variable is the hyperbolic inverse sine of the number of pixels deforested in the cell. ln Price is the log of our crop price index, defined in equation (2). Cover[x] are bins for deciles of forest cover in 2000. With the 50% canopy threshold (columns 1 and 2), the number of observations is reduced compared to the estimates with the 25% canopy threshold as few grid of 0.5 degree do not include any pixels of 30 meters with a 50% canopy cover in 2000.

Table OA.8: Sensitivity analysis of specifications with cell characteristics: canopy threshold & PPML estimator

	(1)	(2)	(3)	(4)
Model	Model 1	Model 2	Model 1	Model 2
Canopy threshold	50%	50%	25%	25%
Estimator	OLS	OLS	PPML	PPML
ln Price	1.248^{a}		1.109^{a}	
	(0.088)		(0.111)	
× ln dist. port	-0.119^{a}	-0.328^{a}	-0.417^{a}	-0.484^{a}
	(0.027)	(0.026)	(0.035)	(0.035)
× ln dist. cap.	0.193^{a}	0.003	0.205^{a}	0.099^{a}
	(0.025)	(0.025)	(0.038)	(0.037)
× night lights in 2000	-0.103^{a}	-0.051^{a}	-0.093^{a}	-0.038^{b}
	(0.017)	(0.015)	(0.018)	(0.017)
× Cover[D1]		0.027		0.110
		(0.112)		(0.164)
× Cover[D2]		0.397^{a}		0.546^{a}
		(0.107)		(0.145)
× Cover[D3]		0.700^{a}		0.511^{a}
		(0.104)		(0.126)
× Cover[D4]		0.760^{a}		0.745^{a}
		(0.103)		(0.128)
× Cover[D5]		1.071^{a}		0.860^{a}
		(0.099)		(0.126)
× Cover[D6]		1.153^{a}		0.788^{a}
		(0.098)		(0.124)
× Cover[D7]		1.506^{a}		0.978^{a}
		(0.098)		(0.119)
× Cover[D8]		1.800^{a}		1.319^{a}
		(0.096)		(0.120)
× Cover[D9]		2.105^{a}		1.575^{a}
		(0.095)		(0.121)
× Cover[D10]		2.455^{a}		1.782^{a}
		(0.099)		(0.143)
Cell FE	Yes	Yes	Yes	Yes
Country × Year FE	Yes	Yes	Yes	Yes
Observations	220122	220122	221006	221006

Note: Least square estimator in columns (1) and (2), PPML in columns (3) and (4). ^{c} significant at 10%; ^{b} significant at 5%; ^{a} significant at 1%. Standard errors clustered at the cell level in parentheses. The dependent variable is the hyperbolic inverse sine of the number of pixels deforested in the cell. ln Price is the log of our crop price index, defined in equation (2). Cover[x] are bins for deciles of forest cover in 2000. ln dist. port is the log of distance from the closest seaport. ln dist. cap. is the log of the distance from the country's capital city at the beginning of the period. night lights is the average amount of nighttime lights emitted in the cell in 2000.

OA2.6.2 Outliers

Table OA.9: Sensitivity analysis of the baseline estimates: dropping outliers

	(1)	(2)	(3)	(4)	(5)	(6)
Model	Model 1	Model 1	Model 1	Model 2	Model 2	Model 2
Sample: Excluded outliers	3 σ	2 σ	1 σ	3 σ	2 σ	1 σ
ln Price	1.116^a	0.994^a	0.905^a			
	(0.072)	(0.061)	(0.042)			
$\times$ Cover[D1]				-0.245^a	-0.259^a	-0.430^a
				(0.093)	(0.077)	(0.052)
$\times$ Cover[D2]				0.417^a	0.346^a	0.181^a
				(0.085)	(0.073)	(0.049)
$\times$ Cover[D3]				0.691^a	0.574^a	0.465^a
				(0.083)	(0.070)	(0.048)
$\times$ Cover[D4]				0.728^a	0.617^a	0.419^a
				(0.082)	(0.071)	(0.048)
$\times$ Cover[D5]				0.931^a	0.835^a	0.680^a
				(0.082)	(0.070)	(0.047)
$\times$ Cover[D6]				0.977^a	0.877^a	0.732^a
				(0.082)	(0.071)	(0.048)
$\times$ Cover[D7]				1.207^a	1.095^a	0.920^a
				(0.082)	(0.070)	(0.048)
$\times$ Cover[D8]				1.410^a	1.297^a	1.113^a
				(0.079)	(0.068)	(0.047)
$\times$ Cover[D9]				1.651^a	1.503^a	1.352^a
				(0.078)	(0.067)	(0.046)
$\times$ Cover[D10]				1.987^a	1.854^a	1.628^a
				(0.080)	(0.069)	(0.047)
Cell FE	Yes	Yes	Yes	Yes	Yes	Yes
Country $\times$ Year FE	Yes	Yes	Yes	Yes	Yes	Yes
Observations	217908	210305	171382	217913	210312	171342

Note: Least square estimator. ^{c} significant at 10%; ^{b} significant at 5%; ^{a} significant at 1%. Standard errors clustered at the cell level in parentheses. The dependent variable is the hyperbolic inverse sine of the number of pixels deforested in the cell. ln Price is the log of our crop price index, defined in equation (2). Cover[x] are bins for deciles of forest cover in 2000.

Table OA.10: Sensitivity analysis of specifications with cell characteristics: dropping outliers

	(1)	(2)	(3)	(4)	(5)	(6)
Model	Model 1	Model 1	Model 1	Model 2	Model 2	Model 2
Sample: Excluded outliers	3 σ	2 σ	1 σ	3 σ	2 σ	1 σ
ln Price	0.995^{a}	0.888^{a}	0.802^{a}			
	(0.082)	(0.071)	(0.048)			
$\times$ ln dist. port	-0.264^{a}	-0.266^{a}	-0.190^{a}	-0.676^{a}	-0.646^{a}	-0.547^{a}
	(0.064)	(0.055)	(0.037)	(0.062)	(0.055)	(0.037)
$\times$ ln dist. cap.	0.469^{a}	0.445^{a}	0.350^{a}	0.037	0.021	-0.046
	(0.061)	(0.053)	(0.035)	(0.060)	(0.052)	(0.035)
$\times$ night lights in 2000	-0.041^{a}	-0.036^{a}	-0.030^{a}	-0.026^{a}	-0.020^{a}	-0.017^{a}
	(0.006)	(0.005)	(0.003)	(0.005)	(0.005)	(0.003)
$\times$ Cover[D1]				0.051	0.025	-0.138^{b}
				(0.100)	(0.085)	(0.057)
$\times$ Cover[D2]				0.716^{a}	0.627^{a}	0.470^{a}
				(0.094)	(0.081)	(0.054)
$\times$ Cover[D3]				0.991^{a}	0.852^{a}	0.754^{a}
				(0.090)	(0.078)	(0.053)
$\times$ Cover[D4]				1.024^{a}	0.895^{a}	0.704^{a}
				(0.090)	(0.078)	(0.053)
$\times$ Cover[D5]				1.238^{a}	1.123^{a}	0.966^{a}
				(0.090)	(0.077)	(0.052)
$\times$ Cover[D6]				1.276^{a}	1.161^{a}	1.020^{a}
				(0.090)	(0.078)	(0.054)
$\times$ Cover[D7]				1.512^{a}	1.380^{a}	1.218^{a}
				(0.090)	(0.078)	(0.054)
$\times$ Cover[D8]				1.756^{a}	1.624^{a}	1.455^{a}
				(0.091)	(0.079)	(0.054)
$\times$ Cover[D9]				2.030^{a}	1.864^{a}	1.713^{a}
				(0.092)	(0.080)	(0.055)
$\times$ Cover[D10]				2.386^{a}	2.231^{a}	2.002^{a}
				(0.096)	(0.083)	(0.057)
Cell FE	Yes	Yes	Yes	Yes	Yes	Yes
Country $\times$ Year FE	Yes	Yes	Yes	Yes	Yes	Yes
Observations	217898	210295	171419	217912	210298	171388

Note: Least square estimator. ^{c} significant at 10%; ^{b} significant at 5%; ^{a} significant at 1%. Standard errors clustered at the cell level in parentheses. The dependent variable is the hyperbolic inverse sine of the number of pixels deforested in the cell. ln Price is the log of our crop price index, defined in equation (2). Cover[x] are bins for deciles of forest cover in 2000. ln dist. port is the log of distance from the closest seaport. ln dist. cap. is the log of the distance from the country's capital city at the beginning of the period. night lights is the average amount of nighttime lights emitted in the cell in 2000.

OA2.6.3 Dropping large players

Table OA.11: Sensitivity analysis of the baseline estimates: dropping countries with a large crop market share

	(1)	(2)	(3)	(4)	(5)	(6)
Model	Model 1	Model 1	Model 1	Model 2	Model 2	Model 2
Sample: Excluded	Top 10%	Top 25%	Top 50%	Top 10%	Top 25%	Top 50%
ln Price	1.449^a	1.449^a	0.921^a			
	(0.095)	(0.095)	(0.128)			
× Cover[D1]				0.115	0.115	-0.164
				(0.125)	(0.125)	(0.159)
× Cover[D2]				0.709^a	0.709^a	0.288^c
				(0.115)	(0.115)	(0.152)
× Cover[D3]				0.926^a	0.926^a	0.746^a
				(0.112)	(0.112)	(0.147)
× Cover[D4]				0.934^a	0.934^a	0.867^a
				(0.111)	(0.111)	(0.150)
× Cover[D5]				1.178^a	1.178^a	0.966^a
				(0.107)	(0.107)	(0.145)
× Cover[D6]				1.247^a	1.247^a	1.113^a
				(0.107)	(0.107)	(0.146)
× Cover[D7]				1.456^a	1.456^a	1.320^a
				(0.110)	(0.110)	(0.150)
× Cover[D8]				1.692^a	1.692^a	1.470^a
				(0.104)	(0.104)	(0.143)
× Cover[D9]				1.947^a	1.947^a	1.568^a
				(0.101)	(0.101)	(0.139)
× Cover[D10]				2.384^a	2.384^a	1.849^a
				(0.105)	(0.105)	(0.153)
Cell FE	Yes	Yes	Yes	Yes	Yes	Yes
Country × Year FE	Yes	Yes	Yes	Yes	Yes	Yes
Observations	171990	171990	87624	171990	171990	87624

Note: Least square estimator. ^{c} significant at 10%; ^{b} significant at 5%; ^{a} significant at 1%. Standard errors clustered at the cell level in parentheses. The dependent variable is the hyperbolic inverse sine of the number of pixels deforested in the cell. ln Price is our crop price index, defined in equation (2). Cover[x] are bins for deciles of forest cover in 2000. In columns (1) and (4), we dropped the top 10% of the countries with respect to their average market share in our sample's crops post-2000 (top 25% in columns (2) and (5) and top 50% in columns (3) and (6)). The crops considered to compute the market shares are those included in our analysis: banana, barley, cocoa, coconut, coffee, cotton, maize, oil palm, rice, sorghum, soybean, sugar, tea, tobacco, wheat.

Table OA.12: Sensitivity analysis of specifications with cell characteristics: dropping countries with a large crop market share

	(1)	(2)	(3)	(4)	(5)	(6)
Model	Model 1	Model 1	Model 1	Model 2	Model 2	Model 2
Sample: Excluded	Top 10%	Top 25%	Top 50%	Top 10%	Top 25%	Top 50%
ln Price	1.449^a	1.449^a	0.921^a			
	(0.095)	(0.095)	(0.128)			
× Cover[D1]				0.115	0.115	-0.164
				(0.125)	(0.125)	(0.159)
× Cover[D2]				0.709^a	0.709^a	0.288^c
				(0.115)	(0.115)	(0.152)
× Cover[D3]				0.926^a	0.926^a	0.746^a
				(0.112)	(0.112)	(0.147)
× Cover[D4]				0.934^a	0.934^a	0.867^a
				(0.111)	(0.111)	(0.150)
× Cover[D5]				1.178^a	1.178^a	0.966^a
				(0.107)	(0.107)	(0.145)
× Cover[D6]				1.247^a	1.247^a	1.113^a
				(0.107)	(0.107)	(0.146)
× Cover[D7]				1.456^a	1.456^a	1.320^a
				(0.110)	(0.110)	(0.150)
× Cover[D8]				1.692^a	1.692^a	1.470^a
				(0.104)	(0.104)	(0.143)
× Cover[D9]				1.947^a	1.947^a	1.568^a
				(0.101)	(0.101)	(0.139)
× Cover[D10]				2.384^a	2.384^a	1.849^a
				(0.105)	(0.105)	(0.153)
Cell FE	Yes	Yes	Yes	Yes	Yes	Yes
Country × Year FE	Yes	Yes	Yes	Yes	Yes	Yes
Observations	171990	171990	87624	171990	171990	87624

Note: Least square estimator. ^{c} significant at 10%; ^{b} significant at 5%; ^{a} significant at 1%. Standard errors clustered at the cell level in parentheses. The dependent variable is the hyperbolic inverse sine of the number of pixels deforested in the cell. ln Price is our crop price index, defined in equation (2). Cover[x] are bins for deciles of forest cover in 2000. In columns (1) and (4), we dropped the top 10% of the countries with respect to their average market share in our sample's crops post-2000 (top 25% in columns (2) and (5) and top 50% in columns (3) and (6)). ln dist. port is the log of distance from the closest seaport. ln dist. cap. is the log of the distance from the country's capital city at the beginning of the period. night lights is the average amount of nighttime lights emitted in the cell in 2000.

OA2.6.4 Conley standard errors

Table OA.13: Sensitivity analysis of the baseline estimates: Conley's standard errors

	(1)	(2)	(3)	(4)
Model	Model 1	Model 2	Model 1	Model 2
Spatial threshold	500km	500km	1000km	1000km
ln Price	1.267^{a}		1.267^{a}	
	(0.307)		(0.372)	
× Cover[D1]		-0.136		-0.136
		(0.319)		(0.371)
× Cover[D2]		0.566^{c}		0.566^{c}
		(0.297)		(0.340)
× Cover[D3]		0.866^{a}		0.866^{a}
		(0.292)		(0.330)
× Cover[D4]		0.877^{a}		0.877^{a}
		(0.292)		(0.329)
× Cover[D5]		1.115^{a}		1.115^{a}
		(0.294)		(0.338)
× Cover[D6]		1.177^{a}		1.177^{a}
		(0.296)		(0.337)
× Cover[D7]		1.409^{a}		1.409^{a}
		(0.304)		(0.347)
× Cover[D8]		1.594^{a}		1.594^{a}
		(0.302)		(0.350)
× Cover[D9]		1.837^{a}		1.837^{a}
		(0.302)		(0.359)
× Cover[D10]		2.153^{a}		2.153^{a}
		(0.318)		(0.372)
Cell FE	Yes	Yes	Yes	Yes
Country × Year FE	Yes	Yes	Yes	Yes
Observations	221184	221184	221184	221184

Note: Least square estimator. ^{c} significant at 10%; ^{b} significant at 5%; ^{a} significant at 1%. Conley (1999) standard errors allowing for infinite serial correlation and spatial correlation within a 500km or 1000km radius. The dependent variable is the hyperbolic inverse sine of the number of pixels deforested in the cell. ln Price is the log of our crop price index, defined in equation (2). Cover[x] are bins for deciles of forest cover in 2000.

Table OA.14: Sensitivity analysis of specifications with cell characteristics: Conley standard errors

	(1)	(2)	(3)	(4)
Model	Model 1	Model 2	Model 1	Model 2
Spatial threshold	500km	500km	1000km	1000km
ln Price	1.220^a		1.220^a	
	(0.310)		(0.369)	
× ln dist. port	-0.293	-0.703^a	-0.293	-0.703^a
	(0.190)	(0.182)	(0.200)	(0.187)
× ln dist. cap.	0.367^b	-0.038	0.367^c	-0.038
	(0.183)	(0.165)	(0.210)	(0.182)
× night lights in 2000	-0.040^a	-0.023^b	-0.040^a	-0.023^b
	(0.010)	(0.009)	(0.010)	(0.010)
ln Price*Cover[D1]		0.210		0.210
		(0.329)		(0.386)
ln Price*Cover[D2]		0.909^a		0.909^b
		(0.311)		(0.357)
ln Price*Cover[D3]		1.204^a		1.204^a
		(0.307)		(0.349)
ln Price*Cover[D4]		1.212^a		1.212^a
		(0.306)		(0.347)
ln Price*Cover[D5]		1.458^a		1.458^a
		(0.309)		(0.357)
ln Price*Cover[D6]		1.520^a		1.520^a
		(0.310)		(0.356)
ln Price*Cover[D7]		1.756^a		1.756^a
		(0.318)		(0.365)
ln Price*Cover[D8]		1.997^a		1.997^a
		(0.318)		(0.370)
ln Price*Cover[D9]		2.276^a		2.276^a
		(0.320)		(0.381)
ln Price*Cover[D10]		2.621^a		2.621^a
		(0.334)		(0.396)
Cell FE	Yes	Yes	Yes	Yes
Country × Year FE	Yes	Yes	Yes	Yes
Observations	221184	221184	221184	221184

Note: Least square estimator. ^{c} significant at 10%; ^{b} significant at 5%; ^{a} significant at 1%. Standard errors clustered at the cell level in parentheses. The dependent variable is the hyperbolic inverse sine of the number of pixels deforested in the cell. ln Price is the log of our crop price index, defined in equation (2). Cover[x] are bins for deciles of forest cover in 2000. ln dist. port is the log of distance from the closest seaport. ln dist. cap. is the log of the distance from the country's capital city at the beginning of the period. night lights is the average amount of nighttime lights emitted in the cell in 2000.

OA2.6.5 Lagged effect

Table OA.15: Sensitivity analysis of the baseline estimates: lags

	(1)	(2)	(3)	(4)
Model	Model 1	Model 1	Model 1	Model 2
ln Price	1.267^a		1.030^a	
	(0.088)		(0.098)	
ln Price: average t to $t-2$		1.915^a		
		(0.154)		
ln Price: $t-1$			0.330^a	
			(0.096)	
ln Price: $t-2$			0.694^a	
			(0.113)	
ln Price: average t to $t-2$ × Cover[D1]				0.253
				(0.176)
ln Price: average t to $t-2$ × Cover[D2]				1.261^a
				(0.165)
ln Price: average t to $t-2$ × Cover[D3]				1.614^a
				(0.163)
ln Price: average t to $t-2$ × Cover[D4]				1.724^a
				(0.164)
ln Price: average t to $t-2$ × Cover[D5]				1.964^a
				(0.159)
ln Price: average t to $t-2$ × Cover[D6]				2.080^a
				(0.159)
ln Price: average t to $t-2$ × Cover[D7]				2.344^a
				(0.162)
ln Price: average t to $t-2$ × Cover[D8]				2.632^a
				(0.158)
ln Price: average t to $t-2$ × Cover[D9]				3.000^a
				(0.158)
ln Price: average t to $t-2$ × Cover[D10]				3.469^a
				(0.162)
Cell FE	Yes	Yes	Yes	Yes
Country × Year FE	Yes	Yes	Yes	Yes
Observations	221184	196608	196608	196608

Note: Least square estimator. ^{c} significant at 10%; ^{b} significant at 5%; ^{a} significant at 1%. Standard errors clustered at the cell level in parentheses. The dependent variable is the hyperbolic inverse sine of the number of pixels deforested in the cell. ln Price is the log of our crop price index, defined in equation (2). ln Price: average t to $t-2$ is the average price from t to $t-2$.

Table OA.16: Sensitivity analysis of specifications with cell characteristics: lags

Model	(1) Model 1	(2) Model 2
ln Price: average t to $t-2$	1.738^{a}	
	(0.152)	
× ln dist. port	-0.130^{a}	-0.360^{a}
	(0.032)	(0.031)
× ln dist. cap	0.317^{a}	0.098^{a}
	(0.029)	(0.029)
× night lights in 2000	-0.090^{a}	-0.034^{c}
	(0.019)	(0.018)
ln Price: average t to $t-2$ × Cover[D1]		0.154
		(0.174)
ln Price: average t to $t-2$ × Cover[D2]		1.162^{a}
		(0.164)
ln Price: average t to $t-2$ × Cover[D3]		1.512^{a}
		(0.162)
ln Price: average t to $t-2$ × Cover[D4]		1.635^{a}
		(0.162)
ln Price: average t to $t-2$ × Cover[D5]		1.889^{a}
		(0.158)
ln Price: average t to $t-2$ × Cover[D6]		1.992^{a}
		(0.157)
ln Price: average t to $t-2$ × Cover[D7]		2.268^{a}
		(0.160)
ln Price: average t to $t-2$ × Cover[D8]		2.631^{a}
		(0.158)
ln Price: average t to $t-2$ × Cover[D9]		3.039^{a}
		(0.159)
ln Price: average t to $t-2$ × Cover[D10]		3.536^{a}
		(0.164)
Cell FE	Yes	Yes
Country × Year FE	Yes	Yes
Observations	196608	196608

Note: Least square estimator. ^{c} significant at 10%; ^{b} significant at 5%; ^{a} significant at 1%. The dependent variable is the hyperbolic inverse sine of the number of pixels deforested in the cell. ln Price is the log of our crop price index, defined in equation (2). ln Price: average t to $t-2$ is the average price from t to $t-2$. ln dist. port is the log of distance from the closest seaport. ln dist. cap. is the log of the distance from the country's capital city at the beginning of the period. night lights is the average amount of nighttime lights emitted in the cell in 2000.

OA2.6.6 Baseline results by continent

Table OA.17: Baseline results by continent

	(1)	(2)	(3)	(4)	(5)	(6)
Model	Model 1	Model 2	Model 1	Model 2	Model 1	Model 2
Continent	Africa		America		Asia	
ln Price	0.393^b		1.839^a		0.569^b	
	(0.190)		(0.110)		(0.228)	
× Cover[D1]		-0.979^a		1.025^a		-0.260
		(0.209)		(0.198)		(0.244)
× Cover[D2]		-0.236		0.906^a		0.523^b
		(0.205)		(0.159)		(0.235)
× Cover[D3]		0.419^b		0.771^a		0.863^a
		(0.208)		(0.135)		(0.244)
× Cover[D4]		0.526^b		0.816^a		0.810^a
		(0.209)		(0.132)		(0.244)
× Cover[D5]		0.724^a		1.083^a		1.030^a
		(0.205)		(0.129)		(0.234)
× Cover[D6]		0.797^a		1.064^a		1.159^a
		(0.208)		(0.129)		(0.233)
× Cover[D7]		1.023^a		1.374^a		1.146^a
		(0.204)		(0.132)		(0.240)
× Cover[D8]		0.979^a		1.671^a		1.420^a
		(0.202)		(0.119)		(0.249)
× Cover[D9]		1.030^a		2.041^a		1.573^a
		(0.206)		(0.116)		(0.237)
× Cover[D10]		1.135^a		2.463^a		1.301^a
		(0.207)		(0.118)		(0.287)
Cell FE	Yes	Yes	Yes	Yes	Yes	Yes
Country × Year FE	Yes	Yes	Yes	Yes	Yes	Yes
Observations	73692	73692	91116	91116	56232	56232

Note: Least square estimator with cell and country × year fixed effects. ^{c} significant at 10%; ^{b} significant at 5%; ^{a} significant at 1%. Standard errors clustered at the cell level in parentheses. The dependent variable is the hyperbolic inverse sine of the number of pixels deforested in the cell. ln Price is the log of our crop price index, defined in equation (2). Cover[x] are bins for deciles of forest cover in 2000.

OA2.6.7 Controlling for time-varying covariates

Table OA.18: Controlling for precipitation and temperature

	(1) Model 1	(2) Model 1	(3) Model 2
ln Price	1.267^a	1.237^a	
	(0.088)	(0.087)	
Average temperature		0.237^a	0.224^a
		(0.022)	(0.022)
Average precipitation		-0.000^a	-0.000^a
		(0.000)	(0.000)
ln Price*Cover[D1]			-0.163
			(0.113)
ln Price*Cover[D2]			0.549^a
			(0.104)
ln Price*Cover[D3]			0.853^a
			(0.102)
ln Price*Cover[D4]			0.862^a
			(0.100)
ln Price*Cover[D5]			1.097^a
			(0.097)
ln Price*Cover[D6]			1.152^a
			(0.097)
ln Price*Cover[D7]			1.380^a
			(0.098)
ln Price*Cover[D8]			1.562^a
			(0.094)
ln Price*Cover[D9]			1.800^a
			(0.092)
ln Price*Cover[D10]			2.112^a
			(0.095)
Cell FE	Yes	Yes	Yes
Country × Year FE	Yes	Yes	Yes
Observations	221184	221184	221184

Note: Least square estimator with cell and country × year fixed effects. ^{c} significant at 10%; ^{b} significant at 5%; ^{a} significant at 1%. Standard errors clustered at the cell level in parentheses. The dependent variable is the hyperbolic inverse sine of the number of pixels deforested in the cell. ln Price is the log of our crop price index, defined in equation (2). Cover[x] are bins for deciles of forest cover in 2000. Average temperature and Average precipitation are the yearly average temperature and precipitation of the cell, respectively.

Figure OA.12: Controlling for average suitability

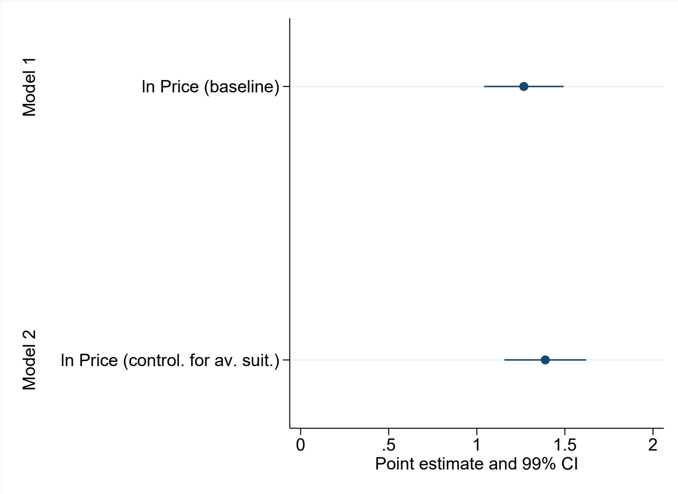

Note: Point estimates and confidence intervals for the effect of the crop price index on deforestation. Model 1 is the baseline estimate of the effect while Model 2 controls for average cell suitability interacted with year dummies. Horizontal lines represent 99% confidence intervals.

OA2.6.8 Relative deforestation: percent of 2000 forest cover

Figure OA.13: Relative deforestation: percent of 2000 forest cover

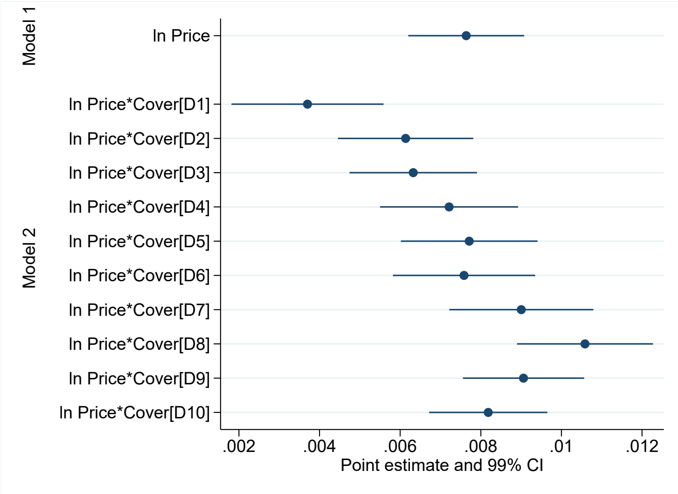

Note: Point estimates and confidence intervals for the effect of the crop price index on deforestation. Model 1 is the baseline estimate of the effect while Model 2 allows the effect of crops on the share of deforested pixels (relative to forest cover in 2000) to vary across deciles of forest cover as of 2000. Horizontal lines represent 99% confidence intervals.

OA2.6.9 Considering meat and pasture, rangeland, and grassland

For our baseline price index and baseline estimations, we choose to concentrate on agricultural crops, and do not include meat, because meat production does not rely on land as strongly and systematically as production of agricultural crops. Beef can be produced on or off the grassland. When beef is produced off the grassland, it is fed hay or grain that is transported to the beef production site. Thus, the place where the beef is raised and the place where the grass grows is not always the same. This is a major difference with crop production. In addition, we do not have direct data on "beef suitability" but rather indirect data on the type of soil that can be consumed by beef as food.

With these remarks in mind, we replicate here our estimations with a revised price index that considers beef markets. More precisely, we use GAEZ suitability data for alfalfa, pasture and grass together with data on the world price of beef from the World Bank. We build the modified price index as follows. We first add the suitability of alfalfa, pasture and grass to have a measure of "beef suitability" for each cell c, $S_c^{16} = S_c^{alfalfa} + S_c^{pasture} + S_c^{grass}$. We then compute the relative suitability of each crop $i = 1, ..., 15$ and beef $i = 16$:

$$\alpha_c^i = \frac{S_c^i}{\sum_{j=1}^{16} S_c^j}. \tag{OA.5}$$

Then, for each cell c and year t, we compute our modified price index of crops and beef based on the cell-specific relative suitability of each crop and beef:

$$\text{Price}_{c,t} = \sum_{i=1}^{16} \alpha_c^i \times P_t^i, \tag{OA.6}$$

Figures OA.14 and OA.15 and Tables OA.19 and OA.20 display the results.

Figure OA.14: Baseline effects of crop prices on deforestation (incl. meat)

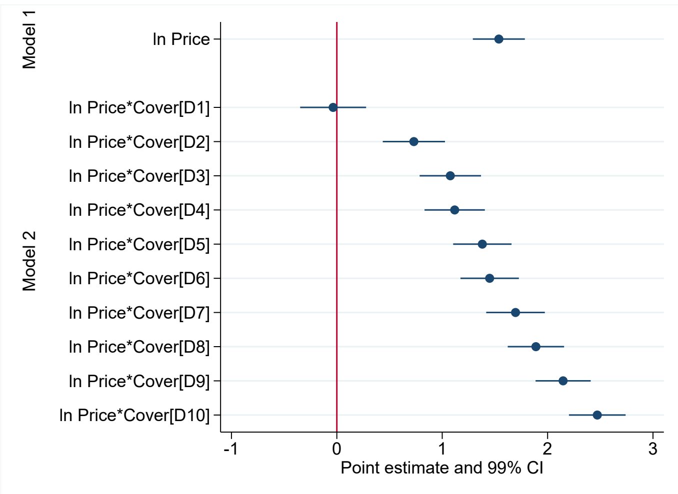

Note: Point estimates and confidence intervals for the effect of the crop price index on deforestation. The crop price index includes meat prices, and the relative suitability of alfalfa, pasture and grass used as measure of meat suitability. Model 1 is the baseline estimate of the effect while Model 2 allows the effect to vary across deciles of forest cover as of 2000. Horizontal lines represent 99% confidence intervals.

Table OA.19: Baseline results (incl. meat)

	(1) Model 1	(2) Model 2
ln Price	1.537^a	
	(0.096)	
× Cover[D1]		-0.035
		(0.121)
× Cover[D2]		0.731^a
		(0.115)
× Cover[D3]		1.077^a
		(0.113)
× Cover[D4]		1.118^a
		(0.111)
× Cover[D5]		1.381^a
		(0.107)
× Cover[D6]		1.450^a
		(0.108)
× Cover[D7]		1.696^a
		(0.108)
× Cover[D8]		1.889^a
		(0.104)
× Cover[D9]		2.147^a
		(0.102)
× Cover[D10]		2.472^a
		(0.104)
Cell FE	Yes	Yes
Country × Year FE	Yes	Yes
Observations	221184	221184
Period	2001-2018	2001-2018

Note: Least square estimator. ^{c} significant at 10%; ^{b} significant at 5%; ^{a} significant at 1%. Standard errors clustered at the cell level in parentheses. The dependent variable is the hyperbolic inverse sine of the number of pixels deforested in the cell. Ln Price is the log of our crop price index, defined in equation (2). Cover[x] are bins for deciles of forest cover in 2000. The crop price index includes meat prices, with share of alfalfa, pasture and grass suitability used as measure of meat suitability.

Figure OA.15: Cell-level characteristics (incl. meat)

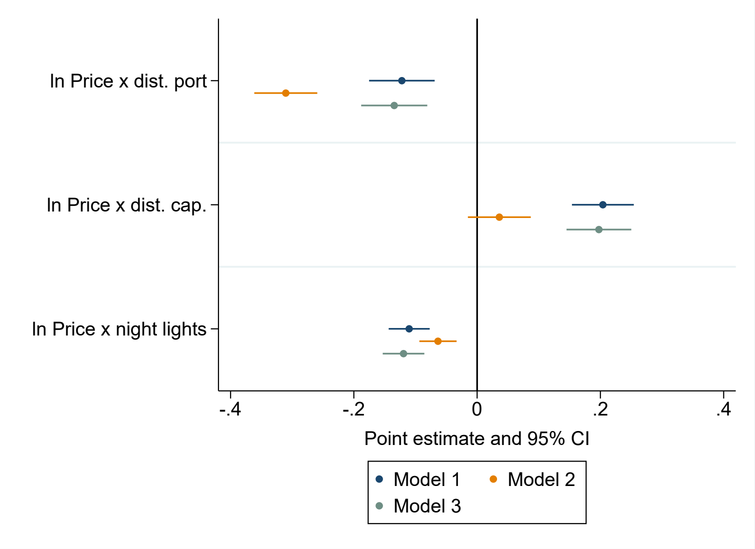

Note: The figure displays the point estimates and confidence interval of the effect of the interaction between cell-specific characteristics and our price index. The crop price index includes meat prices, and the relative suitability of alfalfa, pasture and grass used as measure of meat suitability. The effect of crop price on deforestation is not reported here. Model 1 uses the baseline specification, augmented with interaction terms between the price index and (standardized) cell-characteristic variables (see Section 3). Model 2 allows the effect of crop price on deforestation to vary across the deciles of the initial forest cover distribution. Model 3 controls for a full set of interaction terms between country dummies and the price index.

Table OA.20: Baseline results with cell characteristics (incl. meat)

	(1) Model 1	(2) Model 2	Model 3
ln Price	1.406[a]		
	(0.096)		
× ln dist. port	-0.122[a]	-0.310[a]	-0.134[a]
	(0.027)	(0.026)	(0.027)
× ln dist. cap.	0.204[a]	0.036	0.198[a]
	(0.026)	(0.026)	(0.027)
× night lights in 2000	-0.110[a]	-0.064[a]	-0.119[a]
	(0.017)	(0.015)	(0.017)
× Cover[D1]		-0.094	
		(0.121)	
× Cover[D2]		0.671[a]	
		(0.114)	
× Cover[D3]		1.013[a]	
		(0.112)	
× Cover[D4]		1.061[a]	
		(0.110)	
× Cover[D5]		1.337[a]	
		(0.107)	
× Cover[D6]		1.399[a]	
		(0.107)	
× Cover[D7]		1.654[a]	
		(0.107)	
× Cover[D8]		1.919[a]	
		(0.105)	
× Cover[D9]		2.222[a]	
		(0.103)	
× Cover[D10]		2.580[a]	
		(0.108)	
Cell FE	Yes	Yes	Yes
Country × Year FE	Yes	Yes	Yes
Country FE × price	No	No	Yes
Observations	221184	221184	221184
Period	2001-2018	2001-2018	2001-2018

Note: Least square estimator. [c] significant at 10%; [b] significant at 5%; [a] significant at 1%. Standard errors clustered at the cell level in parentheses. The dependent variable is the hyperbolic inverse sine of the number of pixels deforested in the cell. ln Price is the log of our crop price index, defined in equation (2). Cover[x] are bins for deciles of forest cover in 2000. ln dist. port is the log of distance from the closest seaport. ln dist. cap. is the log of the distance from the country's capital city at the beginning of the period. night lights is the average amount of nighttime lights emitted in the cell in 2000. The crop price index includes meat prices, with share of alfalfa, pasture and grass suitability used as measure of meat suitability.

OA2.7 Global and local prices: correlations

Figure OA.16: Local and word prices

(a) Maize (b) Rice (c) Sorghum (d) Wheat

Source: Porteous (2019) and World Bank.

Table OA.21: Correlation local prices and world prices

	(1)	(2)	(3)	(4)	(5)
Dep. var.			Local price		
World price	0.659[a]	0.610[a]	0.694[a]	0.689[a]	0.960[a]
	(0.023)	(0.032)	(0.026)	(0.036)	(0.074)
Sample (crops included)	All	Maize	Rice	Sorghum	Wheat
Market FE	Yes	Yes	Yes	Yes	Yes
Crop FE	Yes	No	No	No	No
Observations	3292	1403	868	873	145

Note: Least square estimator. [c] significant at 10%; [b] significant at 5%; [a] significant at 1%. Data on local prices are from Porteous (2019). Local price is the log of the local market price. World price is the log of the international price.